FH Aachen
University of Applied Science
Jülich Campus

FH AACHEN
UNIVERSITY OF APPLIED SCIENCES

European Master of Science in Nuclear Applications

Determination of polonium evaporation from liquid lead-bismuth eutectic by the transpiration method

By

Joachim Schnitzler

Jülich, August 2012

This master thesis work has been carried out at SCK•CEN, Advanced Nuclear Systems, Chemistry and Conditioning Programme in collaboration with FH Aachen University of Applied Sciences, Jülich Campus, Department of Chemistry and Biotechnology.

This thesis has been supervised by:

Dr. Alexander Aerts
SCK•CEN
Advanced Nuclear Systems
Chemistry and Conditioning Programme

Prof. Dr. Ulrich W. Scherer
FH Aachen University of Applied Sciences, Jülich Campus
Department of Chemistry and Biotechnology

This thesis is my own independent work and is the result of my sole efforts. No other sources or references have been used in its production apart from the ones quoted.

Jülich, _ _ _ _ _ _ _ _ _ _

Abstract

Lead-bismuth eutectic (LBE) applied as coolant and spallation target causes formation of Po-210 by neutron activation of Bi-209. For licensing and safety assessment of MYRRHA knowledge about the evaporation behaviour of polonium from lead-bismuth eutectic is of high importance. Polonium evaporation from LBE was investigated by a small number of groups. Results of their measurements are not in a good agreement and the conditions of these experiments were not all specific to MYRRHA.

In the present work evaporation of Po-210 from LBE was investigated with the transpiration method. Ar/5% H_2 was used as carrier gas and LSC measurement was used to determine the Po content before and after evaporation. The distribution of Po in LBE samples was measured after diluting Po containing LBE with inactive LBE, showing that Po is homogeneously distributed inside the sample. Kinetic experiments showed evaporation close to ideal exponential release. The change of the cover gas to 100% Ar had no significant influence on the evaporation behaviour. From temperature dependent experiments an apparent Henry constant correlation was derived, showing a good agreement with one of three different correlations from literature. Flow rate dependent experiments were performed with and without insertions to investigate where saturated conditions can be achieved. It remains unclear if the saturated region is quite narrow. The insertions showed no influence on saturation. Evaporation of Po in presence of Pt in the LBE was investigated as noble metals were assumed to bind Po and therefore hinder the evaporation.

Content

1. Introduction

Nuclear power accounts for an important share of energy production of most industrial countries. Since the accidents of Three Mile Island, Chernobyl and Fukushima, safety aspects of nuclear power generation and safety of nuclear waste disposal have become the focus of the discussion.

In future reactor concepts liquid lead-bismuth eutectic (LBE) is considered as a coolant having several safety advantages compared to water. Moreover, LBE can serve as a target material for spallation sources where neutrons are produced by bombarding heavy nuclei with high energy protons which makes an accelerator driven nuclear system cooled with LBE possible.

The Multi hYbrid Research Reactor for High-tech Application (MYRRHA) which is under development in the Belgian Nuclear Research Center (SCK•CEN) is intended to be the first LBE cooled subcritical Accelerator Driven System (ADS).

A disadvantage of LBE cooled nuclear systems is the activation of the coolant leading to the formation of significant amounts of polonium in the coolant. In a reactor most of the polonium will stay dissolved in LBE but a fraction will volatilize into the cover gas, presenting an important safety issue.

Volatile polonium consists of aerosols and molecular species. Due to its high radiotoxicity, volatile polonium is a potential problem during standard operation of the reactor and in accidental cases. Therefore, knowledge about the polonium volatilization is crucial for developing safety measures like filter systems and to assess radiological impact of various accident scenarios.

To date, relatively few data are available on the volatilization of polonium from LBE. The purpose of the present work is to quantitatively determine the equilibrium volatility of polonium in LBE. The thermochemical quantity that describes this equilibrium is the vapor pressure.

The vapor pressure of polonium in LBE was measured with variation of crucial parameters such as temperature. The kinetics of Po evaporation were investigated. Results are discussed and compared with literature data. An outlook for further steps on investigations will be given.

1.1. MYRRHA

Since its foundation in 1952 the Belgian Nuclear Research Center (SCK•CEN) in Mol has been at the forefront in the development of innovative nuclear facilities. The BR2 [BR2] reactor which is in operation since 1962 is one of the flagships of SCK•CEN and was mainly used for material testing for fission and fusion reactors, fuel research, reactor safety and production of medical radioisotopes. The operation license of the BR2 will expire in 2016 but can be prolonged until 2026. Since 1998 SCK•CEN is working on the MYRRHA project in order to replace the BR2 reactor. It is foreseen to start the construction in 2020 and the first operation in 2023.

MYRRHA is designed as an Accelerator Driven System (ADS) which means that a high energy proton beam is delivered to a lead-bismuth spallation target which is linked to a sub-critical reactor. Without proton beam the reactor has no self-sustaining chain fission reaction like common nuclear power reactors. The additional neutrons necessary to sustain nuclear fission are produced by the spallation reaction on the lead-bismuth target. As spallation target materials high mass elements and alloys like Pb, Hg and LBE are favoured because the spallation yield increases in general with increasing mass. Lead-bismuth eutectic is also the primary coolant inside the MYRRHA reactor.

Whereas most reactors use neutrons which are moderated to thermal energies MYRRHA is a reactor with a fast neutron spectrum. In this context, MYRRHA is intended to be a demonstrator for the so called Lead-Cooled Fast Reactor (LFR) which is one of the six Generation IV (GenIV) future reactor types selected by the Generation IV International Forum. GenIV reactor concepts are intended to be more economically due to higher fuel efficiency and they are inherently safe and proliferation resistant. MYRRHA is also designed for various research purposes, such as transmutation studies, irradiation studies of materials for fusion and medical radioisotope production [De Bruyn2011].

A model of the MYRRHA reactor vessel is shown in Fig. 1 (a). The proton beam tube with the support plates and the core barrel is in the centre of the vessel. On the sides of the central structure, coolant pumps and behind, heat exchangers are shown. For the purpose of the present work, the MYRRHA reactor can be simplified as shown in Fig. 1 (b). In the reactor vessel, the liquid phase consists of 4000 tonnes of LBE at a maximal temperature of about 400 °C. Above this LBE a gas plenum is present with a volume of about 100 m^3. The cover gas will be Ar, containing trace levels of oxygen only. Impurities formed by activation and

spallation in LBE will show the tendency to partition between LBE and cover gas, ultimately reaching equilibrium concentrations. The equilibrium between components dissolved in the LBE and the gas phase is indicated by the arrows in Fig. 1 (b). More volatile components such as Hg will show higher equilibrium concentrations in the gas phase. The estimated equilibrium of Po based on literature data is discussed below in Section 1.5.

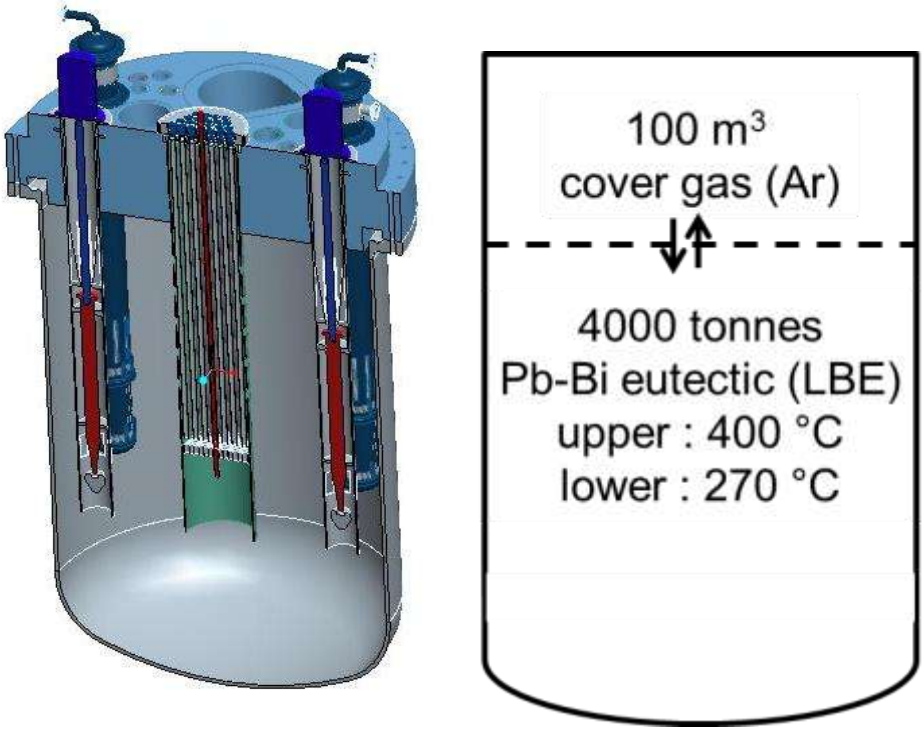

Fig. 1. (a) Model of the MYRRHA reactor vessel **(b)** simplified model of the MYRRHA reactor vessel showing the exchange of components between liquid LBE and the cover gas.

1.2. Lead-Bismuth Eutectic: physicochemical properties and its application as coolant

Lead-bismuth eutectic (LBE) consists of 45.5wt-% Pb and 55.5wt-% Bi. At this composition, the alloy forms an eutectic with a melting point of approximately 125 °C.

Naturally lead occurs with the four stable isotopes Pb-204, Pb-206, Pb-207 and Pb-208. Bismuth occurs naturally just as the isotope Bi-209 with a very long half-life of $\approx 1.9*10^{19}$ years. Due to its extremely long half-life bismuth can be considered as stable.

LBE has been applied in nuclear systems in the USA and Russia already in 1950's. Russia has used LBE-cooled fast reactor technology extensively in their submarines [Zrodnikov1999].

Applied as coolant, LBE has the advantages that it has a high boiling point, good heat conductivity and can be considered as inert regarding reactions with water, at least compared to sodium. Applied in ADS, LBE provides a high neutron yield in spallation reactions with high energy protons and has low scattering and absorption cross-sections with fast neutrons. Furthermore LBE has a high self shielding ability which reduces the emission of ionizing radiation.

One disadvantage of LBE beside coolant activation is that it dissolves components of structural materials leading to embrittlement. LBE induced corrosion can be avoided by control of the dissolved oxygen concentration in LBE.

1.3. Physicochemical properties of Polonium

Polonium was first discovered by Marie and Pierre Curie while investigating the radioactivity of pitch blend. Marie Curie won the Nobel Prize in Chemistry for the discovery of polonium and radium. Today 34 different isotopes of polonium are known, ranging from Po-186 to Po-220. Polonium has no stable isotope [Magill2006].

Isotopes with half-lifes larger than one day are listed in Table 1. Due to their long half-life, these isotopes are useful for studies of polonium chemistry. In the present work, Po-210 will be used exclusively.

Table 1. Most useful polonium isotopes for chemical investigations, their according half-lifes, and decay modes

Isotope	Half-life	Decay (Energy - ratio)
Po-206	8.8d	β^+ (1.85 MeV – 94.5%); α (5.32 MeV – 5.5%)
Po-208	2.90a	α (5.21 MeV – 99.9%)
Po-209	102a	α (4.97 MeV – 99.9%)
Po-210	138.4d	α (5.40 MeV – 99.9%)

As an element of the chalcogen group, the chemical behaviour of polonium is expected to follow the trend by S, Se and Te [Neuhausen2003]. Polonium is redox amphoteric. The most stable oxidation state is +4. Oxidation states -2, +2 and +6 are less stable. Elemental polonium metal occurs in two different allotropic forms. The α–form is a simple cubic crystal structure. Po is the only element that forms this structure at standard conditions. The β–form is rhombohedral. The melting point is 254°C and the boiling point at ambient pressure is estimated to be 962°C.

Although the physicochemical properties of polonium were investigated for several decades, some properties which are disturbed by radioactive decay are not accurately known today. For example Po-210, which is the most easily produced Po isotope, generates 140 W/g of heat, rendering calorimetric measurement of e.g. phase transitions nearly impossible.

Po-209 with a half-life of 102 years would be a suitable candidate for investigations of macroscopic quantities but its availability is low.

1.4. Polonium production and evaporation in the MYRRHA reactor

Besides separation of polonium from the natural ore, Po-210 is usually produced by neutron irradiation of Bi-209 in a reactor forming Bi-210 by neutron capture and subsequent decay to Po-210:

$$^{209}\text{Bi}\ (n,\gamma)\ ^{210}\text{Bi} \xrightarrow{\beta-} {}^{210}\text{Po} \xrightarrow{\alpha} {}^{206}\text{Pb} \qquad (1)$$

This is also the main production route of Po-210 inside the MYRRHA reactor. A second formation route is by double neutron capture of Pb-208 followed by two β^--decays but the production by direct activation of Bi-209 is several orders of magnitude higher. Mostly due to (p,xn) reactions also other polonium isotopes are formed in MYRRHA. However, these are much less abundant than Po-210 (Fig. 2) [Aerts2011a].

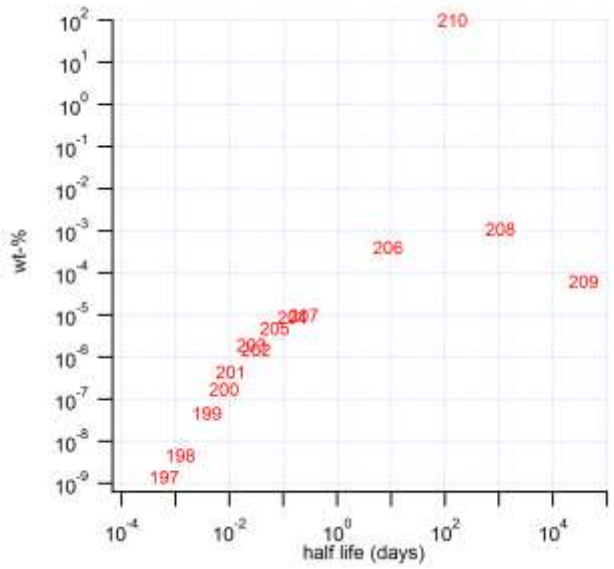

Fig. 2. Distribution of Po isotopes by weight after 90 days of operation versus isotope half-life [Aerts2011a].

The amount of Po-210 in the MYRRHA reactor will reach a steady-state when its production rate equals its decay rate. Due to the operational scheme foreseen for MYRRHA, this steady state will be modulated during operation (90 days) and during shutdown (30 or 90 days) (Fig. 3) [Aerts2011a]. This leads to the appearance of peaks in the graph of the Po content versus operation time. The maximal Po content will be reached for the first time after 750 days of operation and amounts to ca. 2 kg, corresponding to a Po mole fraction of about 10^{-7} in the coolant.

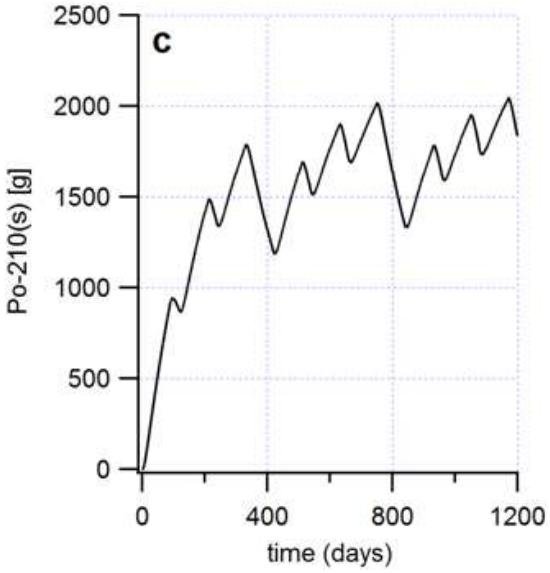

Fig. 3. Amount of dissolved Po in 4000 ton during operation of the MYRRHA reactor [Aerts2011a].

The 2 kg of Po are highly diluted in the LBE but a certain amount of it volatilizes into the cover gas (Fig. 4) [Aerts2011a]. Although the amount is very low this is a safety problem due to its high radiotoxicity. The radiotoxicity of the cover gas can be appraised by comparing it with the maximal allowed concentration (MAC). The MAC value is the concentration of Po-210 that corresponds to a 20 mSv per year dosis by inhalation for a worker, assuming 2000 h/year working time and a breathing rate of 1 m^3/h. In Fig. 4, the maximal allowed concentration (MAC) for gaseous polonium is indicated by the red line. During operation, the MAC value is exceeded by four orders of magnitude. The concentration of gaseous polonium is slightly below the MAC during shut down. As the temperature during shut down is lower than during operation the equilibrium shifts from the side of gaseous polonium to the side of polonium dissolved in LBE. This leads to a decrease of the vapor pressure and gaseous Po-210 concentration.

The calculations for the gaseous polonium amount of Fig. 3 [Aerts2011a] were made by assuming only monoatomic vapor species and ideal gas behaviour, and the vapor pressure correlation by Ohno *et al.* for Po in LBE [Ohno2006], which is considered to be the most reliable one [OECD2011]. For the licensing and safety assessment of MYRRHA it is crucial to have precise and accurate data of the vapor pressure of polonium in LBE. As already mentioned, there exists significant disagreement between various literature data on Po evaporation.

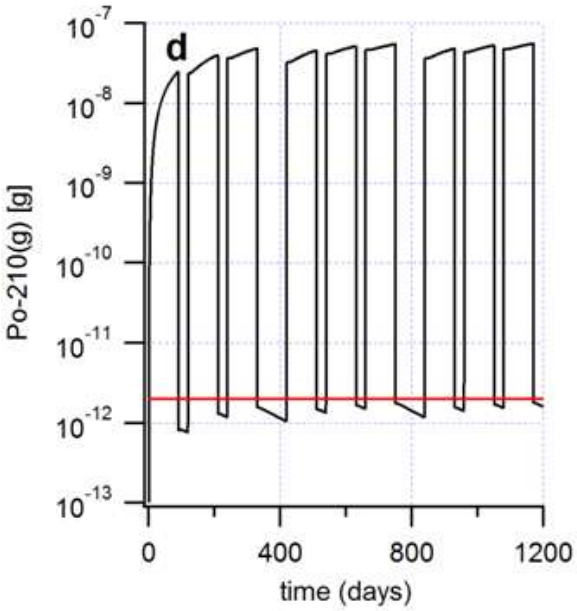

Fig. 4. Amount of gaseous Po-210 in 100m³ cover gas in the MYRRHA reactor vessel. The red line indicates the MAC value for Po-210 [Aerts2011a].

1.5. General concepts of the vapor pressure of dilute solute-solvent systems

1.5.1. Vapor pressure of pure substances

The vapor pressure of a substance is a fundamental thermochemical property. It corresponds to the following equilibrium reaction between a pure compound A in condensed state and that compound in the gaseous state:

$$A_{(cond)} \leftrightarrow A_{(g)} \quad (2)$$

In this simple equilibrium reaction, it is assumed that the substance A evaporates congruently, i.e. the molecules forming the condensed state are equal to those in the gas. This might be not the case for e.g. metal oxides. For example, the vapor phase above Li_2O consists of Li(g), O_2(g) and several gaseous oxides such as Li_2O and Li_3O [Hilpert1990]. Pure Po metal in inert atmosphere evaporates as monomers and dimers [Eichler2002]:

$$Po_{(cond)} \leftrightarrow Po_{(g)} \quad (3)$$

and

$$2Po_{(cond)} \leftrightarrow Po_{2(g)} \quad (4)$$

The equilibrium constant for Eq. 2 is given by

$$K = \frac{p_A / p^{\phi}}{a_{A(cond)}} \quad (5)$$

Here, p_A is the vapor pressure in equilibrium with the condensed phase, $p°$ is the reference pressure (usually 1 bar in thermochemical tables), $a_{A(cond)}$ is the activity of the condensed component A, which is by definition equal to 1 for a pure substances. Taking this into account we obtain

$$K = p_A \quad (6)$$

remembering that the reference pressure is 1 bar. The equilibrium constant is related to the standard Gibbs free energy change of the equilibrium reaction (2):

$$\Delta G = -RT\ln K \qquad (7)$$

Thus, if the equilibrium vapor pressure p_A is measured, the standard Gibbs energy change for the corresponding reaction can be calculated and vice versa. A reaction occurs spontaneously if the associated Gibbs energy change is negative.

1.5.2. Vapor pressure of dissolved trace components

The equilibrium evaporation reaction of a dissolved component in a solvent, here, Po in LBE, is given by:

$$A_{(LBE)} \leftrightarrow A_{(g)} \quad (8)$$

In very dilute solutions the vapor pressure p_A is proportional to its mole fraction x_A, as expressed by Henry's law

$$p_A = K_A \, x_{A(LBE)} \quad (9)$$

where p_A [Pa] is the vapor pressure of pure A and K_A [Pa] is the Henry constant. The meaning of the Henry constant can be understood by expressing it in terms of a thermodynamic activity coefficient $\gamma_{A(LBE)}$, which is the deviation of the activity of the dissolved component from a reference compound, typically the pure component. Thus:

$$K_A = \gamma_{A(LBE)} \, p_A \quad (10)$$

where

$\gamma_{A(LBE)}$ = activity coefficient of compound A in LBE [-]

The activity coefficient may be influenced by compound formation between solute and solvent. For example, in LBE the vapor pressure of polonium is strongly suppressed, probably due to formation of lead and bismuth polonides [Ohno2006; Neuhausen2004]. The activity coefficient of polonium in LBE $\gamma_{Po(LBE)}$ is $\approx 10^{-3}$ at 400 °C. Therefore the vapor pressure of polonium dissolved in LBE is about 1000 times less than that of elemental Po at hypothetical equal concentration at 400 °C.

1.5.3. Temperature dependence of the Henry constant

Like all equilibrium constants, the Henry constant depends on the temperature. To first approximation, its temperature dependence can be given by following equation:

$$K_A = \exp(-A/T+B) \quad (11)$$

A and *B* are empirical constants, which have to be determined experimentally by measurement of the Henry constant at different temperatures. The constants *A* and *B* are related to thermochemical quantities of the equilibrium as follows:

$$K_A = \exp(-\Delta G/(R\,T)) \quad (12)$$

ΔG = Gibbs free energy [J/mol] for the equilibrium described by Eq. 2. The Gibbs free energy is defined as:

$$\Delta G = \Delta H - T\,\Delta S \quad (13)$$

where ΔH is the Enthalpy [J/mol] and ΔS the Entropy [J/mol-K].

By inserting Eq. 12 into Eq. 13 one arrives at

$$K_A = \exp(-\Delta H/(R*T)+\Delta S/R) \quad (14)$$

so $A = \Delta H/R$ correlates to the enthalpy and $B = \Delta S/R$ to the entropy. Therefore by measuring the temperature dependence of the Henry constant (or vapor pressure in case of a pure substance), the enthalpy and entropy changes associated with reaction Eq. 2 can be determined.

From a practical point of view, if the Henry constant (Eq. 11) for Po in LBE is known at different temperatures, the equilibrium concentration of gaseous Po can be calculated for MYRRHA given a concentration of Po in LBE as provided by neutronic calculations. Methods to measure the vapor pressure of Po above LBE and to derive the Henry constant from these measurements are discussed in the following Section.

1.6. Measurement of vapor pressures - the transpiration method

There are several methods to measure low vapor pressures such as those of dissolved trace components. An important technique is Knudsen Effusion Mass Spectrometry (KEMS) allowing to measure vapor pressures between 10^{1}-10^{-8} Pa. In this technique a condensed sample is heated in a small cell until equilibrium vapor pressure is reached. The cell has a small hole of a known diameter were the vapor effuses through, without changing the equilibrium in the cell. The effused vapor particles are then quantified and analyzed by a coupled mass spectrometer [Booth2009]. From effusion rate, the vapor pressure in the cell can be calculated. This technique has the advantage that also the chemical nature of the vapor molecules can be determined. A disadvantage is that the technique is limited to low total pressures. For example, it is typically not possible to measure evaporation in the presence of a cover gas at atmospheric pressure.

Another technique is the so called transpiration method (also called transportation method) [Merten1967], which will be used in the present work to measure vapor pressures of dilute solutions of Po in LBE.

In this method a condensed sample is placed in a boat, which is put inside of a tube. The sample is then heated while a carrier gas flows over it. The carrier gas can be either inert (e.g. Ar) or reactive. The evaporated molecules are transported away from the sample position by the carrier gas. By measuring the amount of transported molecules, the vapor pressure of the sample can be determined.

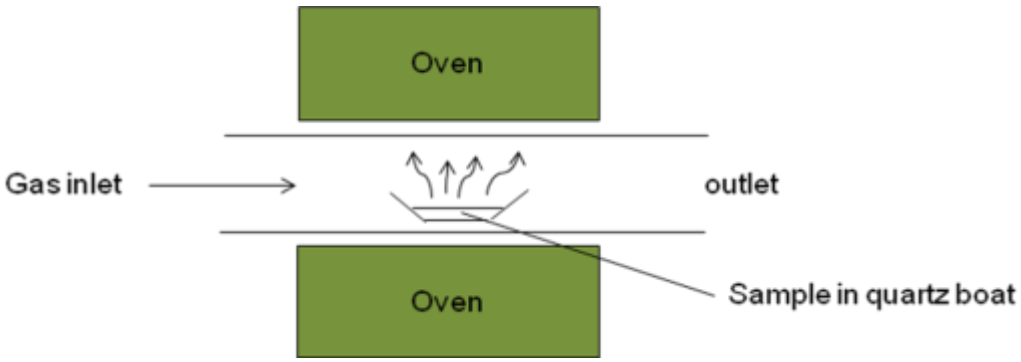

Fig. 5. Schematic drawing of the transpiration method.

An overview of the theoretical background [Aerts2012a] of vapor pressure measurement with the transpiration method is given in this section.

Assuming vapor transport by convection only and that the carrier gas is saturated with vapors, the change of the amount of sample *n* with time due to evaporation is given by following differential equation:

$$\frac{dn}{dt} = -\dot{V} c_{\mathrm{sat}} \tag{15}$$

$\dot{V}$ = volumetric gas flow over the sample [m³/s]
c_{sat} = saturation concentration of vapor in the carrier gas [mol/m³]
n = amount of sample [mol]

By inserting $c_{sat} = p_{sat} / (R\ T)$, i.e. assuming the vapors are ideal, and subsequent integration one gets:

$$n(t) = n(0) - \frac{\dot{V} p_{\mathrm{sat}}}{RT} t \tag{16}$$

n(0) = intial amount of sample [mol]
p_{sat} = saturated vapor pressure [Pa]
R = ideal gas constant [J/(mol*K)]
T = Temperature [K]
t = time [s]

Eq. 16 is a good approximation if the concentration of the dissolved component does not change significantly during the experiments as this equation is only valid for pure samples. The amount of evaporated solute per unit time is proportional to its vapor pressure if the evaporation is under saturated conditions. In contrast to Eq. 16 the saturated vapor pressure is in this case a function of the solute remaining in the sample:

$$\frac{dn}{dt} = -\frac{\dot{V} p_{\mathrm{sat}}(n)}{RT} \tag{17}$$

As the p_{sat} is linear to *n* for dilute solution, described by Henry´s law (Eq. 9, Section 1.5.2.) one gains:

$$\frac{dn}{dt} = -\frac{\dot{V} K n}{RT n_{\mathrm{tot}}} \tag{18}$$

K = Henry constant [Pa]

n_{tot} = total amount of sample [mol]

After integration one obtains:

$$\frac{n(t)}{n(0)} = \exp\left(-\frac{\dot{V} K}{RT n_{\mathrm{tot}}} t\right) \tag{19}$$

n(t) = amount of solute after time t

For some systems, the evaporation of the solvent cannot be neglected, especially for high temperatures. In this case, with increasing time also the total amount of the sample n_{tot} (Eq. 19) will decrease over time. As the Po in LBE is highly diluted, p_{sat} of the solvent and the sample are identical. Therefore, the dependence of the molar amount of the solvent on experiment time is given by Eq. 20.

$$\frac{n(t)}{n(0)} = \left(1 - \frac{\dot{V} p_{\mathrm{sat}} t}{RT n_{\mathrm{tot}}(0)}\right)^{\frac{K}{p_{\mathrm{sat}}}} \tag{20}$$

For the calculation of the apparent Henry constant K from our experiments, the formula has been rearranged to:

$$K = -\frac{p_{\mathrm{lbe}}}{\ln\left(1 - \frac{\dot{V} p_{\mathrm{lbe}} t}{RT m_{\mathrm{lbe}}(0)}\right)} \ln\left[\frac{n(t)}{n(0)}\right] \tag{21}$$

With p_{LBE} as the vapor pressure of LBE [Pa] and m_{LBE} (0) as the initial mass of LBE sample [g][Aerts2012a].

For the vapor pressure determination saturated vapor is crucial. At saturated conditions the vapor concentration is independent from the flow rate of the carrier gas, which leads to a plateau region (Fig. 6). At too high flow rates saturation cannot be achieved as the evaporating vapor is transported very fast away by convective flow. For very low flow rates diffusion is the main contributor to the evaporation and the convective flow is overestimated, leading to the higher value of the mole fraction of vapor.

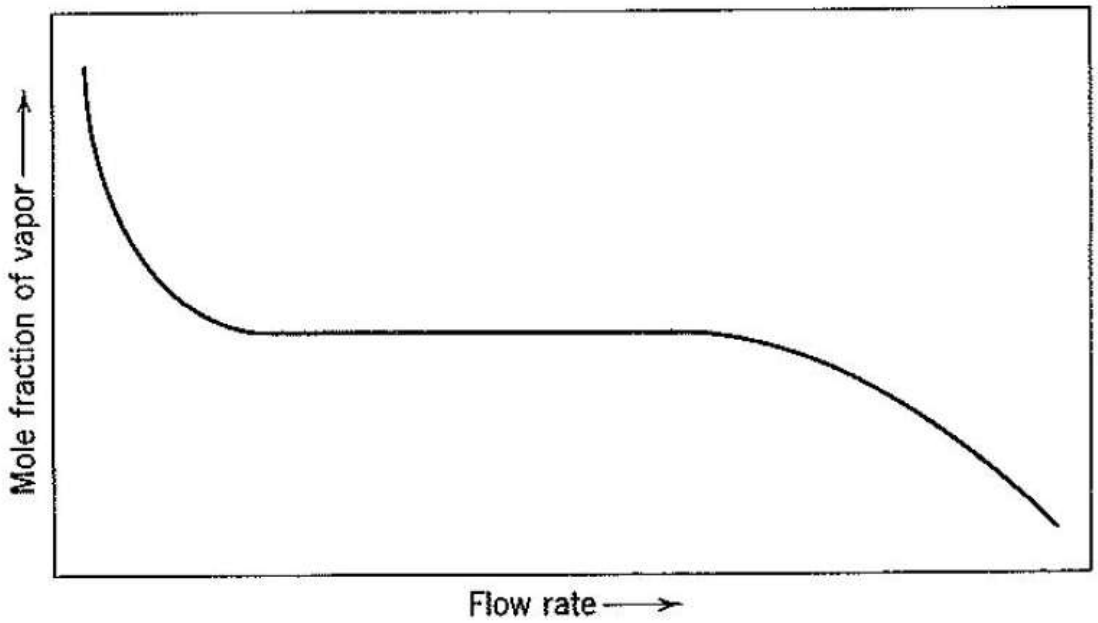

Fig. 6. Variation with the flow rate of the mole fraction of vapor in effluent gas from the transpiration experiment [Merten1967]. The upturn at low flow rates is caused by diffusive transport. In the constant region is the vapor in saturated conditions and independent from the flow rate. The downturn at high flow rates is caused convective transport where saturation cannot be achieved.

Usually in the transpiration method the mass of the condensed vapor or the weight loss of the sample is measured. For our experiments the initial polonium content *n(0)* and after evaporation *n(t)* is measured with LSC (see Section 2.5.) as the activity is proportional to the amount of the radionuclide.

Because the Po content of the sample is determined by measuring activity, information on the chemical nature of the evaporated species is not accessible by this method. For this reason just the apparent Henry constant can be determined and not the true Henry constant over LBE. This approach just takes the total polonium amount in the gas phase into account. By relating the obtained apparent Henry constant to the vapour pressure of pure metallic Po, an activity coefficient for Po in the solution can be received. It is also possible to determine or guess the actual chemical state of Po in the liquid or gas phase and use the vapor pressure with

corrections for the dilution, the non ideal behaviour and experimental thermodynamical data. Both approaches should lead finally to the same result [Jolkkonen2009].

In terms of MYRRHA the total activity in the cover gas is the most important value. It serves as input for the calculation of the amount in the cover gas for equilibrium conditions like standard operation and shut down. Knowledge about the gaseous species of polonium is important for the prediction of polonium evaporation under conditions different from standard operation like water inleakage or change of the cover gas atmosphere as these can influence the vapor pressure of polonium. For example the vapor pressure is lowered when PoO_2 is formed in O_2 containing atmosphere. The different suggested and proposed gaseous polonium species are presented in the following section.

1.7. Gaseous polonium species

The literature according to the volatile polonium species evaporating from LBE is contradictive and different vapor species are assumed or proposed. A short overview is presented in this section.

A thermochemical analysis by Neuhausen *et al.* suggested that metal polonides are probable vapor species above LBE. BiPo seems to be more stable than PbPo [Neuhausen2003, Neuhausen2004]. Experiments done with the polonium homologue Te from Ohno *et al*. revealed that the amount of Te and Pb were equal in the gas phase. Therefore the authors concluded that PbPo is a probable vapor species of polonium above LBE [Ohno2006]. Strong interaction of Po with Pb is also suggested by experiments with lead-gold eutectic [Rizzi2011a] and Li0.17Pb0.83 [Feuerstein1992].

In the experiments on Po evaporation under different gas atmospheres performed by Buongiorno *et al.* it was found that the vapor pressure of Po, as determined by activity measurement, was ten times smaller in pure Ar atmosphere than under a mixed atmosphere of Ar, H_2O and H_2. The increased vapor pressure was attributed to the formation of the very volatile compound H_2Po [Buongiorno2003]. However, this conclusion is contested. Neuhausen *et al*. also performed Po evaporation experiments in the presence of water but no increased vapor pressure was observed [Neuhausen2003]. Also, on the basis of thermochemical arguments, H_2Po is expected to be unstable and therefore its formation is either unlikely or it decomposes fast [Jolkkonen2009]. On the other hand, small amounts of the compound may form as a metastable intermediate in the presence of nascent hydrogen [Bagnall1969].

One indication for this metastable intermediate was observed by thermochromatographic experiments. In thermochromatography a compound is evaporated in a gas stream and adsorbed on a column with a temperature gradient. The more volatile a compound is the lower is its deposition temperature in the column. In the first experiment Po was evaporated in either He or H_2 as carrier gas. Under the H_2 flow Po deposited at colder temperatures then under He. In the second experiment the deposition was investigated at different times under H_2 atmosphere. Po deposited first in a high temperature region (same region from the first experiments under He flow) and migrated with longer experiment time to the colder temperature region [Rizzi2011b].

Although there are indications for the formation of volatile H_2Po and/or other gaseous species over LBE, the true vapor species is still not known.

The vapor pressure depends on the gaseous species and on the chemical interaction of the polonium in its solution which is given by its activity coefficient γ. The activity coefficient is a deviation from a reference state, usually the compound hypothetically dissolved in itself. Activity coefficients of polonium in different lead and bismuth alloys are compared in the LBE handbook [OECD2011]. Additional activity coefficients from literature [Neuhasen2004; Buongiorno2003] were added to this comparison (Fig 7). According to Eq. 10 the activity coefficient is correlated with the Henry constant, therefore the comparison of the activity coefficients is also a comparison of different derived Henry constants. For the calculations of γ a polonium vapor pressure correlation p_{Po} = 10^(-5440 ± 60.0/T +9.46 ± 0.05) from literature [Abakumov1974] was used.

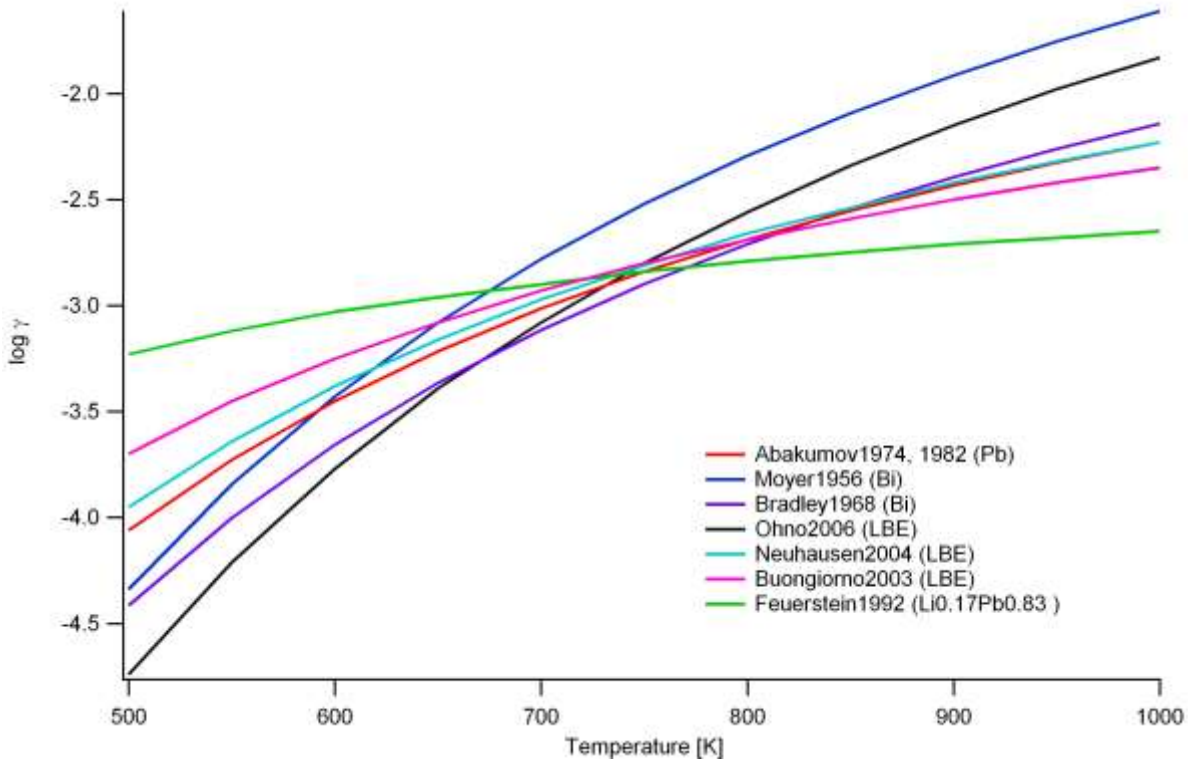

Fig. 7. Activity coefficients for very dilute solutions of Po in liquid Pb and Bi alloys [OECD2011]. (red) as PbPo, as ideal solution in Pb [Abakumov1974, Abakumov1982], (blue) in Bi [Moyer1956], (black) in LBE [Ohno2006], (purple) in Bi Calculated from evaporation data [Bradley1968], (turqoise) in LBE [Neuhausen2004], (magenta) in LBE [Buongiorno2003], (green) in Li0.17Pb0.83 [Feuerstein1992].

It can be generalized that the thermodynamic activity is strongly depressed in all compared Pb and Bi alloys by about two orders of magnitude at 1000 K and even more at low temperatures. In all experiments the Po content in the gas phase was determined by activity measurement.

By comparing the two curves for Po in Bi it is shown that the curve of Bradley *et al.* falls progressively below the curve of Moyer *et al.* The difference between these two is that Bradley *et al.* used non-equilibrium measurement [OECD2011].

The investigations in Li0.17Pb0.83 of Feuerstein *et al.* are assumed to be the least reliable one as their data consists of seven data points with large scattering and the slope of the curve changes significantly when one point is neglected [OECD2011]. Additionally their curve shows the least agreement with the other curves.

Two of the three curves taken from LBE are in a quite good agreement, especially at higher temperatures (Neuhausen *et al.* and Buongiorno *et al.*). Although these two LBE curves are in a good agreement, the third LBE curve of Ohno *et al.* is assumed to be the most reliable one [OECD2011].

The agreement of the curves of Neuhausen *et al.* (Po in LBE) and Abakumov *et al.* (Po in Pb) is remarkable, it can be therefore assumed that Po interacts more strongly with Pb then Bi. The expression for the calculation of the γ from Abakumov *et al.* in the LBE handbook contains a sign error (-0.40 instead of +0.40), however the correct expression was used for the calculation of the curve in the handbook.

The differences between all these data might originate from different used setups, data analysis and different assumptions. It is sometimes not clear how the data was analyzed, where and which assumptions were made and which uncertainties and errors were taken into account.

1.7.1. Sputtering

Besides "chemical" evaporation described in the previous sections, radioactive species can also volatilize into the gas phase by aerosol formation and sputtering. Unlike volatilization by evaporation these processes are not equilibrium processes. Because sputtering is in contrast to evaporation not temperature dependent, it might be an important release mechanism at low temperatures.

Aerosols can be atoms attached to dust particles dispersed in air. In MYRRHA the aerosols are expected to be formed by dispersion of LBE containing polonium or polonium compounds or by condensation of polonium vapors on airborne particles.

Sputtering on the other hand is a consequence of radioactive decay of dissolved elements. One significant property of α-emitting radioactive nuclides is the ability to volatilize even at room temperature. This effect was first observed in 1904 [Brooks1904]. This led to the assumption that the daughter nuclide is recoiled into the opposite direction of the α-particle.

Further investigations showed that also the α-active mother nuclide can be transported by recoil, which could not be explained by the theory of daughter recoil. Therefore the aggregate recoil was assumed, where the daughter nuclide contains a group of undecayed nuclides which are then transported further by diffusion or other decay events. This basic principle, developed in the beginning of last century, is still an accepted theory for the high mobility of Po-210 and other α-decaying nuclides. Though there are still some contradictions which cannot be explained by this theory [Trenn1980].

The term sputtering, coming from particle physics, is also sometimes used in literature which deals with volatility and release of Po. Both effects describe the main process but the origin of the kinetic energy is different [OECD2011].

It is assumed that the fraction of sputtered material or aggregate recoil is higher in reality then in theoretical calculations. Po has the ability to enrich at the sample surface and grain boundaries [Heinitz2010], which can possibly lead to higher release rates caused by sputtering or aggregate recoil.

Although sputtering is an important release mechanism of polonium, investigations on this topic are out of the scope of this work.

1.8. Motivation

Polonium evaporation to the cover gas inside the reactor vessel of MYRRHA is a potential hazard to the people in the near surrounding and the environment in case of an accident or uncontrolled release during maintenance. Due to these facts the evaporation behaviour is a crucial part for the safety assessment and the licensing procedure of the MYRRHA project as the gaseous amount inside the reactor has to be calculated with reliable data. Literature concerning the evaporation behaviour of Po from LBE is scarce and contradictive. Therefore, in the present work evaporation of Po from LBE will be studied by the transpiration method, while systemically verifying whether the assumptions to obtain reliable data with this method are fulfilled. The obtained experience on measurement of Po evaporation will be useful for licensing, design and operation of MYRRHA.

The main goal of the present work is the investigation of evaporation kinetics by variation of evaporation time, the flow rate dependency to verify if saturated vapor can be achieved in the experimental setup and the temperature dependent experiments in order to derive a Henry constant correlation which can be compared with literature data.

These three results should lead to a deeper understanding of the evaporation behaviour of Po from LBE and serve as input for further investigations on this topic and more reliable and available data.

2. Materials and methods

2.1. Production of Po-210/LBE

LBE samples containing Po-210 for evaporation experiments were produced by irradiation of LBE inside the BR-1 reactor. Po-210 is mainly formed by neutron capture of Bi-209 and subsequent β^--decay of Bi-210 (see Section 1.4.).

Cylinder-shape LBE samples with a mass of 2.7 g were irradiated in channel Y4 of the BR-1 reactor for 8 h in a thermal neutron flux of $3.5*10^{11}$ cm^{-2} s^{-1}. The samples were allowed to cool afterwards in a lead container for *ca*. 1 month to let the Bi-210 decay to Po-210. The specific activity of the samples after cooling was about 20 kBq/g.

In the following, the time evolution of the activity of Bi-210 and Po-210 in the sample is calculated (a detailed calculation can be found in the Appendix). The content of Po-210 and Bi-210 in the sample is given by following set of differential equations:

$$dN_{Bi\text{-}210}/dt = k - \lambda_{Bi\text{-}210} * N_{Bi\text{-}210} \quad (22)$$

$$\frac{dN_{Po\text{-}210}}{dt} = N_{Bi\text{-}210} * \lambda_{Bi\text{-}210} - N_{Po\text{-}210} * \lambda_{Po\text{-}210} \quad (23)$$

N_x = number of atoms of nuclide *x* [-]
k = Production rate [s^{-1}]
λ_x = decay constant of of nuclide *x* [s^{-1}]

The term $N_{Bi}*\lambda_{Bi}$ describes the Po-210 formation due to the decay of Bi-210 and the term $N_{Po}*\lambda_{Po}$ describes the decay of the Po-210 itself. Therefore the Po-210 formation due to the decay of Bi-210 can be derived by integration which leads to a Bateman equation:

$$N_{Po\text{-}210}(t) = \left[\frac{\lambda_{Bi\text{-}210}}{\lambda_{Po\text{-}210} - \lambda_{Bi\text{-}210}}\right] * N_{Bi\text{-}210}(0) * [\exp(-\lambda_{Bi\text{-}210} * t) - \exp(-\lambda_{Po\text{-}210} * t)] \quad (24)$$

The equation describes the variation of the number of daughter nuclei with variation of time as consequence of the formation and subsequent decay.
As Bi-209 is the target nuclide for the generation of Bi-210 which then decays to Po-210, the formation of the Bi-210 in a reactor is described by following activation equation:

$$N_{Bi\text{-}210}(0) = \frac{N_{Bi\text{-}209} * \sigma_{Bi\text{-}209} * \Phi * (1 - \exp(-\lambda_{Bi\text{-}210} * t_{irr}))}{\lambda_{Bi\text{-}210}} \quad (25)$$

with $\sigma_{Bi\text{-}209}$ [b] as the neutron capture cross section, Φ [cm^{-2} s^{-1}] the neutron flux and t_{irr} [s] is the irradiation time.

Inserting the activation equation Eq. 24 into Eq. 25 one finally arrives at:

$$N_{Po\text{-}210}(t) = \left[\frac{\lambda_{Bi\text{-}210}}{\lambda_{Po\text{-}210} - \lambda_{Bi\text{-}210}}\right] * \frac{N_{Bi\text{-}209} * \sigma_{Bi\text{-}209} * \Phi * (1 - \exp(-\lambda_{Bi\text{-}210} * t_{irr}))}{\lambda_{Bi\text{-}210}} * [\exp(-\lambda_{Bi\text{-}210} * t) - \exp(-\lambda_{Po\text{-}210} * t)] \quad (26)$$

The maximal Po content after irradiation can be calculated as follows:

$$\lambda_{Bi\text{-}210} * \exp(-\lambda_{Bi\text{-}210} * t) = \lambda_{Po\text{-}210} * \exp(-\lambda_{Po\text{-}210} * t) \quad (27)$$

Yielding the maximal $N_{Po\text{-}210\text{-}max}$ with:

$$t_{max} = \frac{\ln(\lambda_{Po\text{-}210} / \lambda_{Bi\text{-}210})}{(\lambda_{Po\text{-}210} - \lambda_{Bi\text{-}210})} \quad (28)$$

By inserting the decay constants $\lambda_{Po\text{-}210} = 0.00501\ d^{-1}$ and $\lambda_{Bi\text{-}210} = 0.13827\ d^{-1}$ into Eq. 28 one obtains the maximal Po-210 content after $t_{max} = 24.9$d of Bi-210 decay.
The activity of Bi-210 and Po-210 of the samples after irradiation in the BR-1 reactor is shown in Fig. 8. The irradiation of the LBE samples was performed at the 6th of December, 2011. As the present work started in the beginning of March, 2012, the Bi-210 activity was already negligible. The Po-210 activity concentration was about 20 kBq/g.

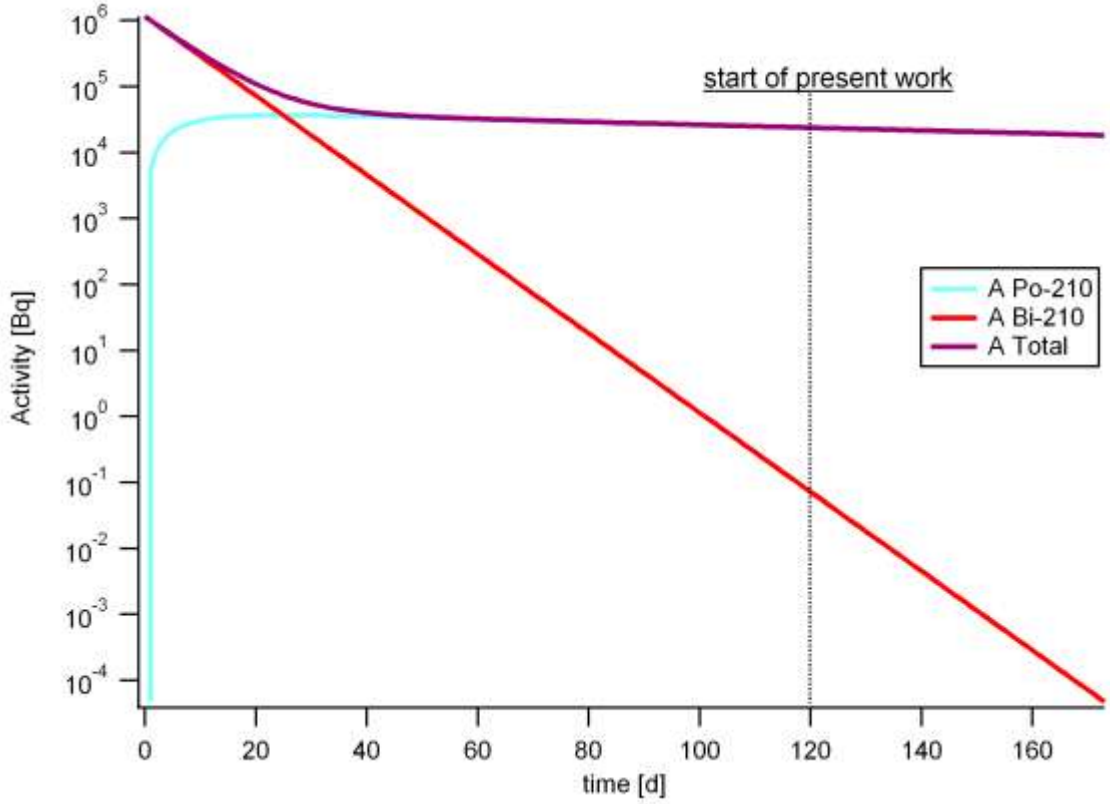

Fig. 8. Time dependency of the activity of Po-210 and Bi-210 after irradiation in BR-1 reactor (t_{irr} = 8 h; $\Phi = 3.5*10^{11}$ cm^{-2} s^{-1}; m_{Target} = 2.7 g LBE; σ = 17 mb).

2.2. Dilution of Po/LBE samples

Evaporation experiments were not performed directly with the irradiated samples described in the previous Section. At the time of the experiments, permission was granted only to do evaporation experiments with samples containing 500 Bq/g Po-210. Therefore, samples after irradiation needed to be diluted with inactive LBE, approximately by a factor 40.

Inactive LBE samples with a mass of about 2.5-2.7 g were cut in half and placed into a quartz sample boat. Between these two pieces, a piece of 50-70mg of Po containing LBE (activity ca. 18 kBq/g, as determined by LSC) was placed. The quartz boat was put into the evaporation setup (see next Section). Before heating, the setup was flushed for 15 minutes with a flow of 1 L/min Ar/5% H_2. The sample was then heated for 30 minutes at 600 °C under the same flow with the same carrier gas, allowing the inactive and active LBE to form a homogeneous melt. The homogeneity of these diluted samples was verified experimentally (See results and discussion, Section 3.1.). Subsequently, diluted samples were solidified by cooling to room temperature.

2.3. Evaporation setup

For evaporation experiments, sample dilution and sample homogenization a transpiration-type setup was used (Fig. 9, 10). The entire setup was placed in a fume hood. Carrier gases were either argon (Air Products) or a mixture of argon with 5% hydrogen (Air Products, Ar 94.994% ± 0.02 % rel., H_2 5 % ± 0.5 % rel.). The flow rate of the carrier gases was controlled by mass flow controllers (Bronkhorst High-Tech B.V., F-201CV-1K0-AGD-33-V). Before entering the sample zone, the carrier gas was purified by a Ni-based filter operating at room temperature (SAES Pure Gas, Inc., MC50-904FV) According to specifications, the filter reduces water and oxygen content of the carrier gas to < 1 ppb.

The purifier is connected via 6 mm stainless steel and perfluoroalkoxy (PFA) tubing to a quartz tube (inner diameter 13 mm) in which the sample is heated. A leak-tight connection with the quartz tube is accomplished by a stainless steel flange with quartz counterflange attached to the quartz tube with Viton o-ring.

To heat the samples to temperatures up to 1000 °C a Carbolite tube furnace, Type 301 was used. The oven is mounted on rails which allows to preheat the oven to the desired temperature away from the sample and then quickly shift the oven to the sample position. This minimizes errors due to warm-up and cooling time.

A rolled copper foil was inserted in the quartz tube after the sample zone to reduce the aerosol formation. To prevent Po escaping the setup a filter filled with activated charcoal (Sigma-Aldrich) and a wash bottle filled with silicon oil were installed downstream from the quartz tube. At the outlet to the fume hood a paper filter was placed to monitor possible contamination.

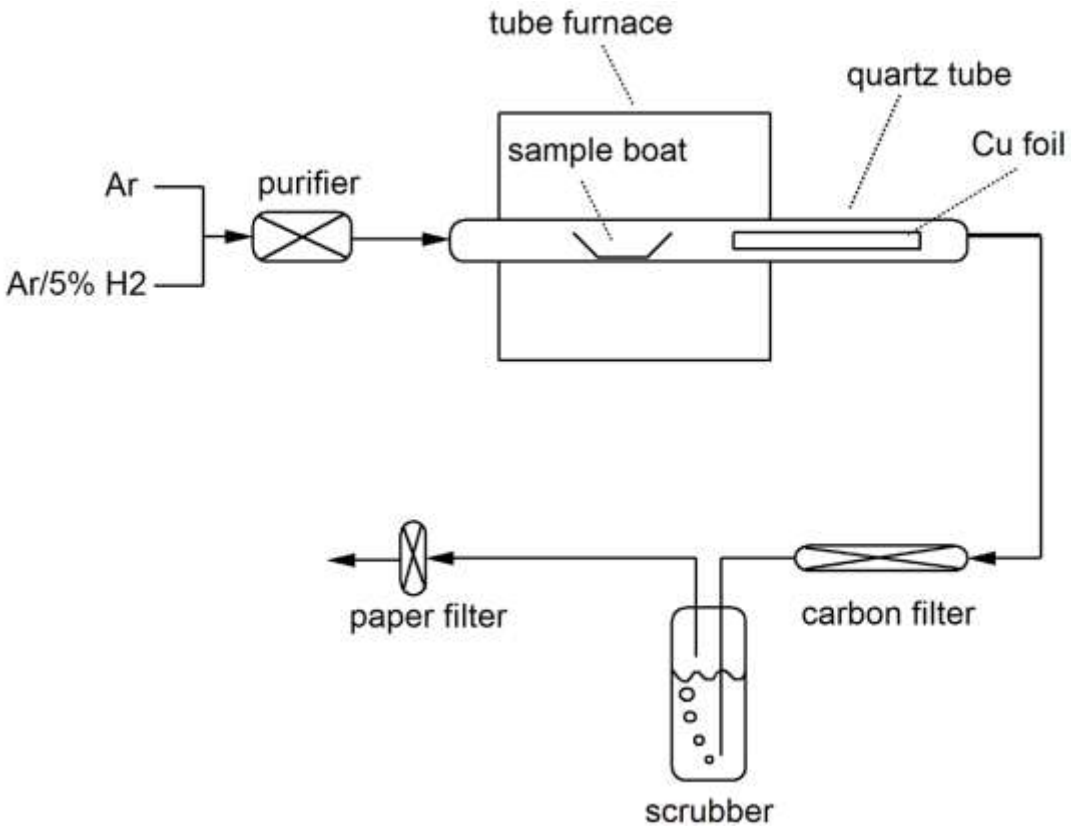

Fig. 9. Schematic drawing of the used evaporation setup.

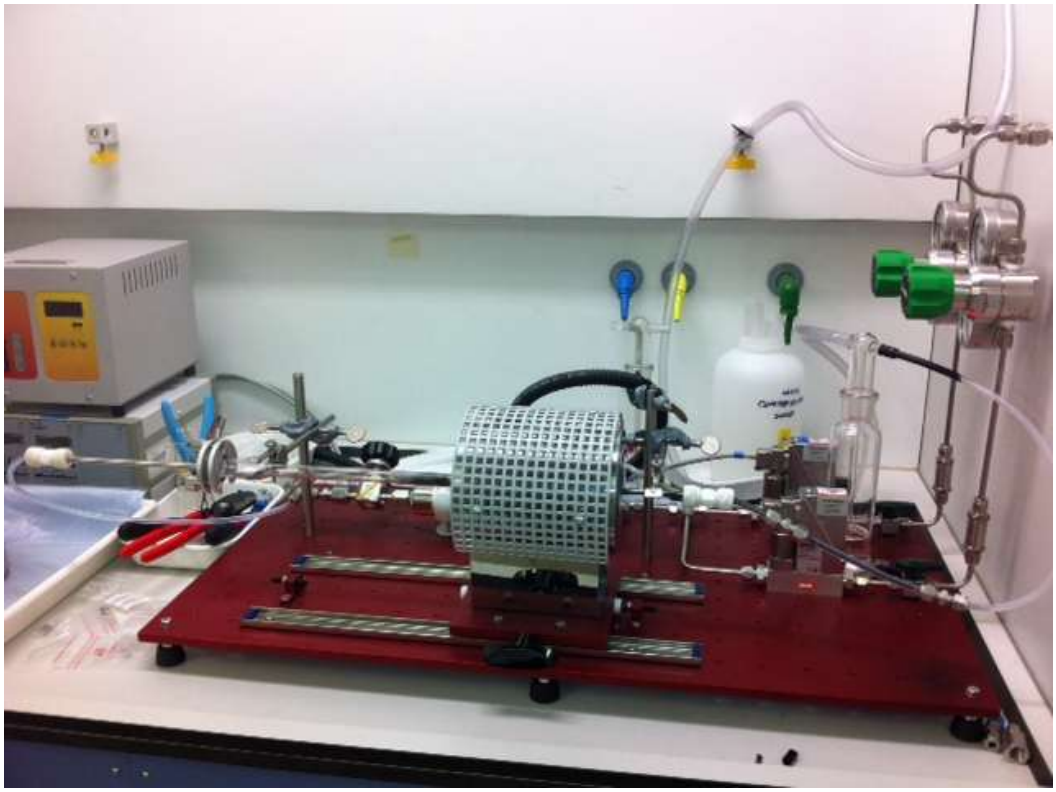

Fig. 10. Picture of the evaporation setup.

2.4. Evaporation experiments

To measure Po evaporation from LBE, the following procedures were followed. Prior to the actual evaporation, the Po/LBE samples were homogenized in order to be able to determine its polonium content reliably. A Po/LBE sample was placed in a quartz sample boat lined with quartz tissue. The quartz boat with sample was inserted in the quartz tube which was then closed and flushed for 15 minutes with a flow of 1 L/min of Ar/5% H_2 to have the setup oxygen free. Afterwards the sample was heated to 600 °C for 30 minutes under the same flow. At this temperature, polonium evaporation is insignificant (see Section 3.3.). After cooling the sample to room temperature it was taken out and cleaned with a tissue which was moisturized with acetone, to remove traces of black Pb and Bi oxides off the sample surface. After this treatment, samples with shiny metallic surfaces were obtained indicating absence of oxides.

After homogenizing the sample, two small subsamples of about 100 mg were cut off the ends of the LBE sample for determination of the initial Po-210 content by LSC measurement. Afterwards the sample is weighted again and put back into the setup which is flushed again for 15 minutes as it was opened and oxygen was able to get into the setup.
The sample was placed accurately in the middle of the tube furnace to ensure maximal temperature with good uniformity over the sample length. Depending on the experimental conditions either the carrier gas flow rate (20 to 1000 mL/min), the oven temperature (600 to 1000 °C) or the evaporation time (2 to 60 min) were varied. After obtaining the desired temperature the oven was moved to the sample location. When the evaporation was finished the oven was removed from sample position and the sample is cooled to room temperature. The Po-210 activity was then again measured by LSC. The difference between initial and final Po activity corresponds to the amount of evaporated Po.

2.5. Liquid Scintillation Counting (LSC)

For the determination of the polonium content in LBE approximately 100 mg were cut off from the LBE with pliers and then weighed with a Sartorius CPA1245 balance. Afterwards the sample was dissolved in 1 mL (7 M) overnight. On the next day the solution was diluted with 6 mL H_2O and homogenised. 2 mL where taken out and put into a plastic LSC vial. 18 mL LSC cocktail (Zinsser Analytic Aquasafe 500Plus) were added and shaken for homogeneity. The LSC sample was counted in a Packard TriCarb 2100TR for 90 minutes each which results in an uncertainty of about 4% for the samples with relatively low activities. As the dissolved LBE gains a yellow colour after some time, probably due to oxidation of the cocktail with the HNO_3, quench measurements were performed with Am-241 and Po-210.
Due to colour quenching, the counting efficiency starts to decrease at a concentration of about 1 g/L dissolved LBE in the LSC sample. In the present work, LSC samples had a concentration of about 1.5-1.7 g/L leading to a counting efficiency of about 85-90%.
In order to gain the net count rate of the polonium, before every LSC measurement a background sample containing 98.6 mg inactive LBE was measured.

2.6. Analysis of LSC data and error analysis

For the data analysis the total count rate over all energies was used because Po-210 is the only radionuclide inside the samples. The error of the count rate is given by:

$$s_r = \frac{\sqrt{M}}{t} \tag{29}$$

with M = total counts and t = measurement time.

The error of the background measurement is similarly given by:

$$s_{r_0} = \frac{\sqrt{M_0}}{t} \tag{30}$$

where M_0 = total counts of the background measurement.

Afterwards the background r_0 is subtracted from the count rate r to obtain the net count rate r_{net}:

$$r_{\text{net}} = r - r_0 \tag{31}$$

And the associated error is:

$$s_{r_{\text{net}}} = \sqrt{\frac{r + r_0}{t}} \tag{32}$$

The weighing error was assumed to be 1 mg absolute and the error on the pipetting volumes was assumed to be 1 % relative [Aerts2011b].

Then the activity A [Bq] of the sample is derived by taking efficiency losses like quenching into account. Then the specific activity A_s [Bq/g] was calculated by dividing the activity with the sample mass m [g]. As the specific activity is proportional to the polonium concentration in LBE e.g. the Henry constant or the fractional release can be calculated by Eq. 21. The errors on the result were calculated using appropriate error propagation formulae.

For Eq. 21 the volume flow $\dot{V}$ is given by the mass flow controller. If necessary the volume flow was corrected for thermal expansion, which leads to a higher flow rate inside tube. The temperature T is set in the oven. The mass m_{LBE} is measured before and after the experiment. The vapor pressure of LBE p_{LBE} is taken from the LBE handbook [OECD2011].

3. Results and Discussion

3.1. Homogeneity of Po/LBE samples after dilution

Before and after the experiments only small samples are taken off from the LBE/Po evaporation sample to determine the Po concentration. In case of heterogeneous distribution the measurement of the Po content would not be representative for the rest of the evaporation sample and would lead to inconsistent results. Therefore verification of a homogeneous polonium distribution inside the LBE is an important step to prove the reliability of our measurements.

For this experiment a small flake of polonium containing LBE (50-70 mg, about 20 kBq/g) was placed in a quartz boat. Left and right of this Po/LBE flake, 1.3 g pieces of inactive LBE were placed. The boat containing the pieces was then heated at 600 °C for 30 minutes under 1000 mL/min Ar/5% H_2 to melt and fuse the LBE pieces. After solidification, the sample was rod-shaped and had a length of *ca*. 150 mm.

The sample was then cut in 10 pieces, each measuring about 1.5 mm. The specific Po activity of each piece was determined by LSC.

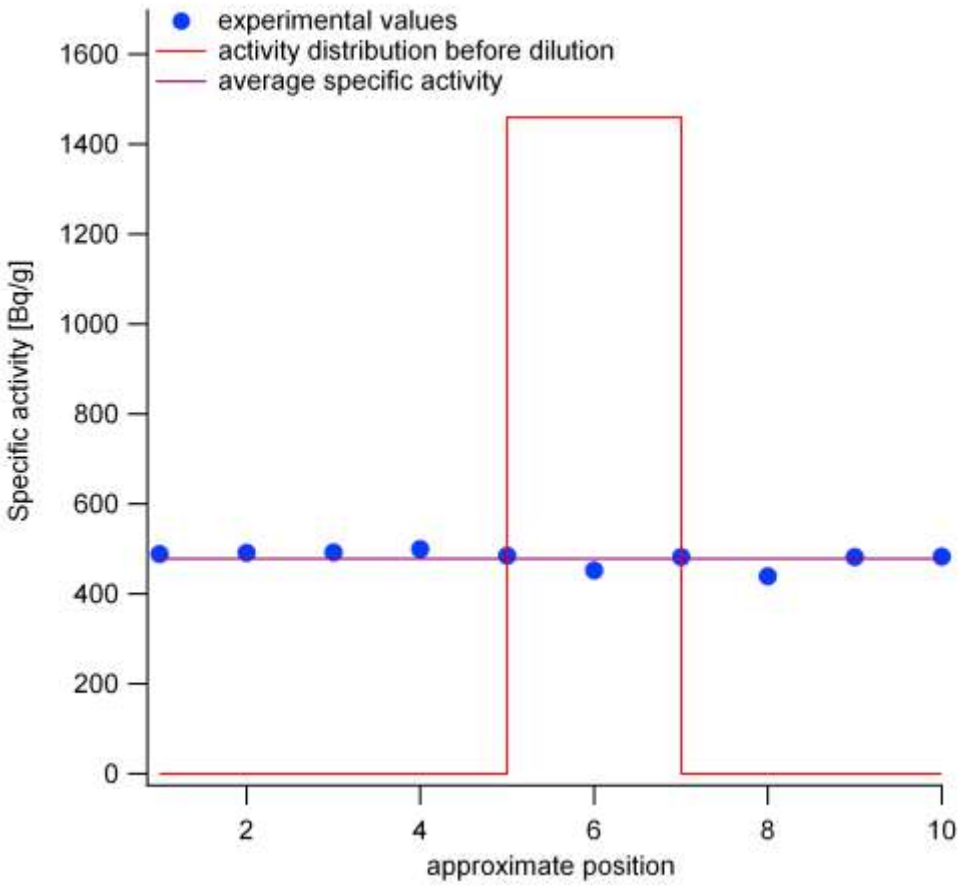

Fig. 11. Specific activity distribution along the length of an LBE sample after dilution. Before melting and dilution, the Po containing sample was in the middle. Pieces of inactive LBE were placed on both sides of it. The approximate distribution of Po before melting and dilution is indicated by the red curve.

Fig. 11 shows the approximate distribution of specific activity along the position of the sample if no homogenization would have occurred (red line, all activity is in the central piece) and the experimentally determined specific activity of the 10 pieces (blue markers). It is clear that during heating polonium has migrated to the left and right of the central Po/LBE flake, resulting in a reasonable degree of homogeneity. From the 10 pieces, an average specific activity of 478 ± 20 Bq/g was determined, corresponding to a standard deviation of about 4%. Po can migrate from the centre of the sample to the ends by two processes: diffusion and convection. Based on the diffusion coefficients of Se and Tl in LBE [OECD2007], a crude estimation of the diffusion velocity of Po in LBE was made by dividing the diffusion coefficient (which is given in $cm^2\ s^{-1}$) with the distance and multiply it with 3600 s/h, giving values between 1-2 mm/h at 600 °C. The diffusion velocity of polonium is expected to be of the same order of magnitude. As our samples have a length of about 1.5 cm it is expected

from the diffusion velocity estimation that diffusion contributes only to small extent to the polonium distribution in LBE. At the high flow rates used during homogenization it was observed that the gas flow caused corrugations on the liquid LBE surface. From this experiment it can be concluded that in samples after dilution Po is homogeneously distributed, probably by the corrugations on the sample surface caused by the gas flow. Therefore cutting of small samples for LSC measurement before and after evaporation are assumed to be representative for the whole LBE sample. Such diluted samples are used for evaporation experiments described in the following section.

3.2. Kinetics of polonium evaporation

Measurements of the fractional release of Po-206 from LBE at different temperatures over time were performed by Neuhausen *et al*. where polonium was evaporated up to 24 days at a maximum temperature of about 700 °C [Neuhausen2004]. As our experiments were performed during one hour of evaporation time at 1000 °C the kinetics of this much shorter evaporation time at higher temperatures had to be investigated to show if the theory for the calculation of the Henry constant (Eq. 21) is in agreement with our experiments.

For these experiments a Po/LBE sample with an initial mass of about 2.5 g Po/LBE was homogenized according to the standard procedure (see Section 2.2.). After flushing the setup, the oven was positioned for the desired evaporation time. After each of this duration the oven was removed to cool down the evaporation sample and a LSC sample of about 100 mg was cut off. Then the procedure was repeated. The sample was heated for following time intervals: 2, 3, 4, 6, 8, 7, 7.5, 7.5, 7.5 and 7.5 minutes.

A first experiment was done with 100% Ar as carrier gas. A second one with Ar/5% H_2.

It was realized that about three minutes were required for the sample to reach stable temperature after positioning the oven around the sample. If a sample is heated only for 2 min it will not reach stable temperature.

Therefore the evaporation sample was heated for 3 minutes at 1000 °C in a third experiment because previous measurements showed that this is the time the sample needs to reach stable temperature. For this preheating and the cooling down afterwards the gas flow was switched off to reduce Po losses. Then the gas flow was switched on to 100 mL/min for the same time intervals as in the previous measurements.

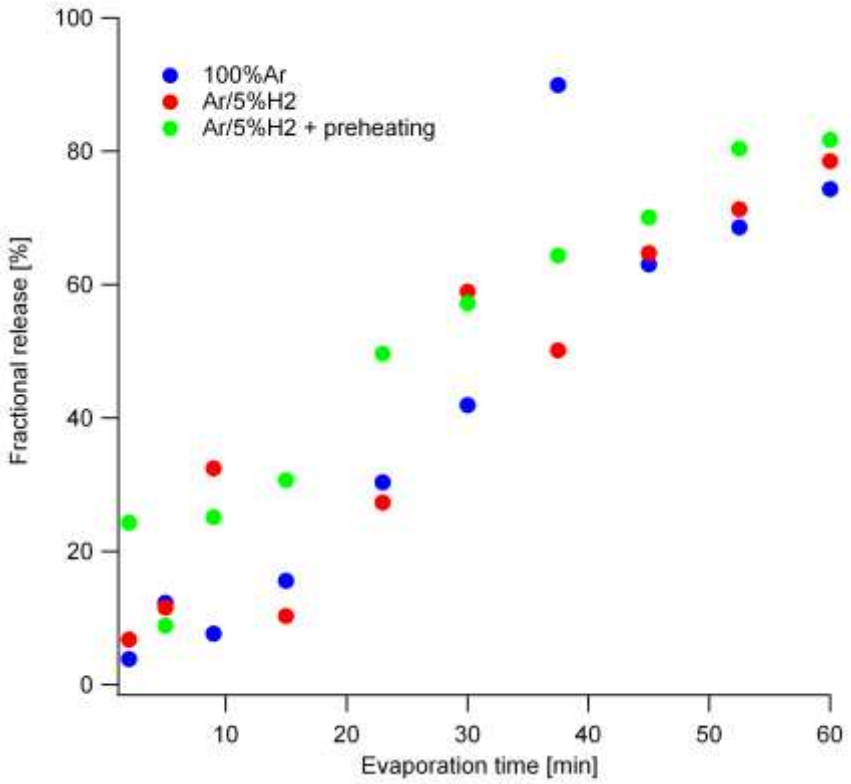

Fig. 12. Fractional release after different evaporation times. The error of the measurements is about 13 % on average.

Fig. 12 shows that the evaporation of Po from LBE without preheating with 100% Ar and Ar/5% H_2 as cover gas have a similar behaviour and the delay time of the two experiments without preheating are not corresponding to the expected fractional release according to Eq. 19. This similarity was unexpected because it was suggested that a possible oxide layer would reduce the evaporation of Po, whereas the oxide layer is reduced under Ar/5% H_2. The sample evaporated under 100% Ar had also a lustreless appearance compared to the other samples.

It can be concluded that there is no or a negligible influence on the evaporation behaviour of Po in 100% Ar or Ar/5% H_2. It is not clear what caused the lustreless appearance on the sample in Ar. Possibly, this is a thin oxide layer, but it does not seem to influence the evaporation of Po.

The measurements performed under Ar/5% H_2 with an additional heat up period show an exponential evaporation curve close to ideal evaporation behaviour. The data of this curve was fitted by rearranging Eq. 20 to

$$\frac{n(t)}{n(0)} = \left(1 - \left(1 - \frac{\dot{V} p_{\mathrm{sat}}\, t}{RT n_{\mathrm{tot}}(0)}\right)^{\frac{K}{p_{\mathrm{sat}}}}\right) \tag{33}$$

The result is shown in Fig. 13. For the fitting the error was weighted with the standard deviation of the points. From the fitting the apparent Henry constant *K* was calculated with *T* = 1273 K, p_{sat} = 276.79 Pa [Abakumov1974], $n_{tot}(0)$ = 0.0119 mol and $\dot{V}$ = 7.1169*10^{-6} m³/s. The value for the flow rate is corrected for the thermal expansion of the carrier gas at 1273 °C. The fitting delivers a value of 8245 ± 606 Pa for the apparent Henry constant K which agrees well with temperature dependent experiments (see Section 3.3.), mentioning that the samples in the temperature dependent experiments were not preheated.

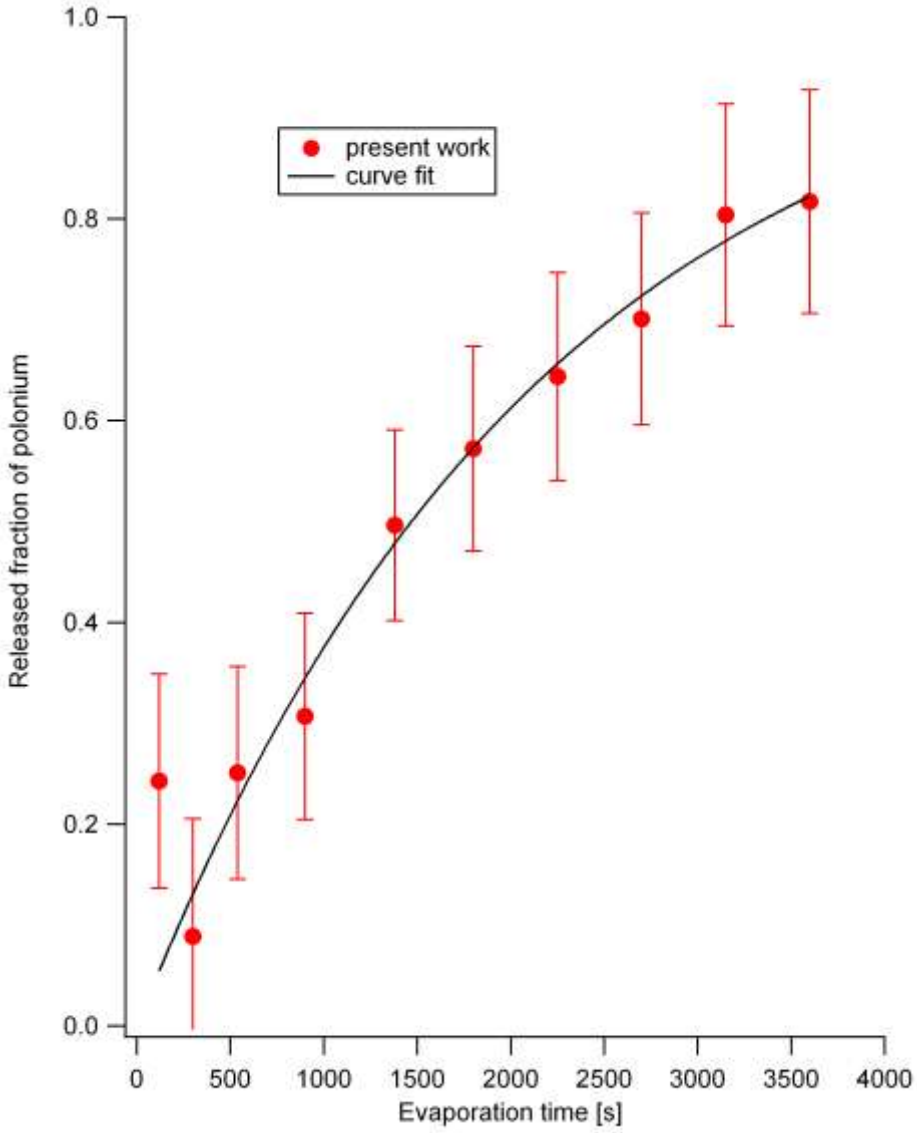

Fig. 13. Release of polonium evaporated from LBE in dependence of total evaporation time at 1000 °C and 100 mL/min STP.

3.3. Temperature dependence of Po vapor pressure

These experiments were performed to investigate the temperature dependence. Therefore the Po evaporation from LBE was measured at different temperatures. The fractional release of polonium was measured between 650 and 1000 °C. The gas flow was constant at $\dot{V}$ = 100 mL/min of Ar/5% H_2, the experiment time t = 1 h. The fractional release is compared with literature data [Neuhausen2004] (Fig. 14).

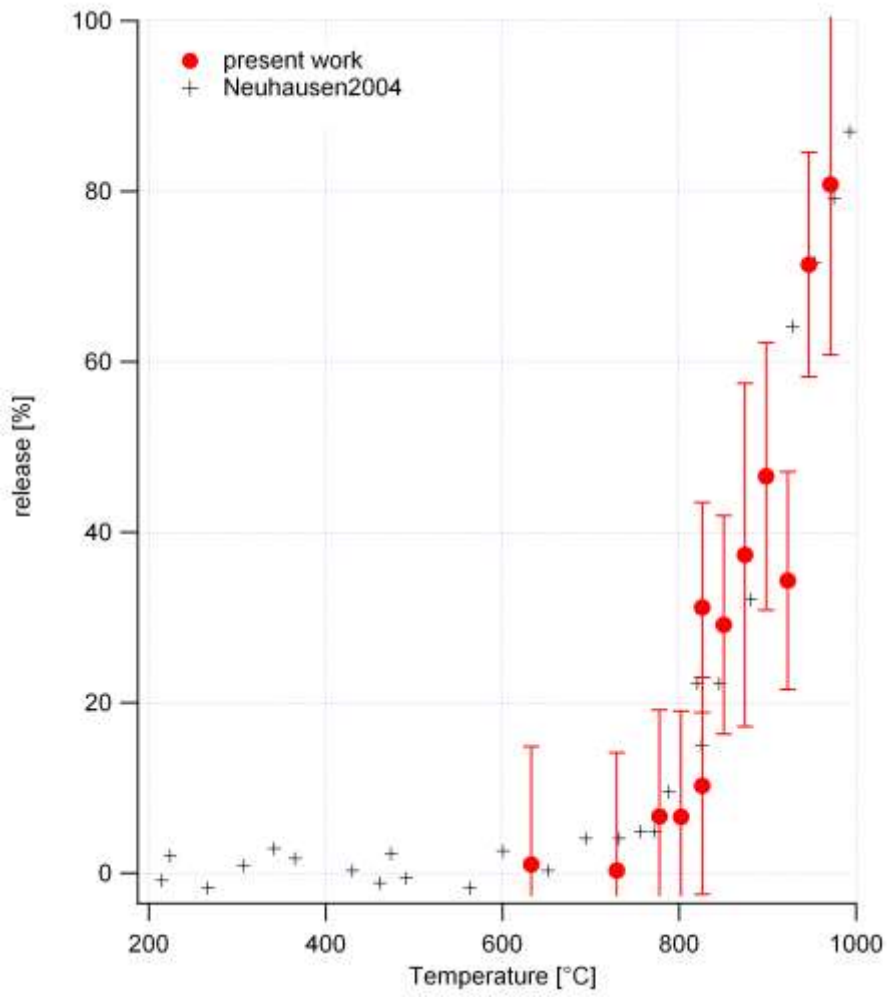

Fig. 14. Fractional release of polonium from LBE at different temperatures (red markers). For comparison: literature data by [Neuhausen2004] (black markers).

The fractional release curve shows that measureable polonium evaporation starts above 600 °C and increases significantly at around 750 °C. At 1000 °C, about 80% of the initially present Po was evaporated. The measured data points are in good agreement with the literature data from Neuhausen *et al*. [Neuhausen2004].

The fractional release depends on the used setup and also on the sample size [Aerts2012a]. By comparing the used sample sizes (present work: 2.5-2.7 g; Neuhausen *et al*.: 0.14 and 0.65 g) our curve should be shifted to higher temperatures. In order to get a better comparison of the obtained data, the Henry constants were calculated for each temperature with Eq. 21. Contrary to the fractional release, the Henry constant is independent from the sample size. As it is not known if our results were obtained with a saturated polonium vapor, the Henry constant that is calculated is actually an apparent value. The apparent Henry constants at different temperatures are shown in Fig. 15.

A temperature correlation for the apparent Henry constants was derived. The temperature coefficients *A* and *B* (Eq. 11) were calculated from a linear curve fit of a plot of the logarithm (base 10) of the Henry constant against 1/T. The coefficient *A* is given by the slope of the graph and the coefficient *B* by the extrapolated intersection point of the curve with the y-axis. The coefficients *A* and *B* (Table 2) and the correlation of the temperature dependent apparent Henry constant (Fig. 15) are compared with literature data.

Table 2. Comparison of coefficients A and B of Henry`s law with literature data

Literature	A	B
Buongiorno2003	-6790 ± 1840	8.46 ± 1.26
Neuhausen2004	-7156	8.9449
Ohno2006	-8348	10.5357
Present work	-8702.1 ± 2380	10.865 ± 1.97

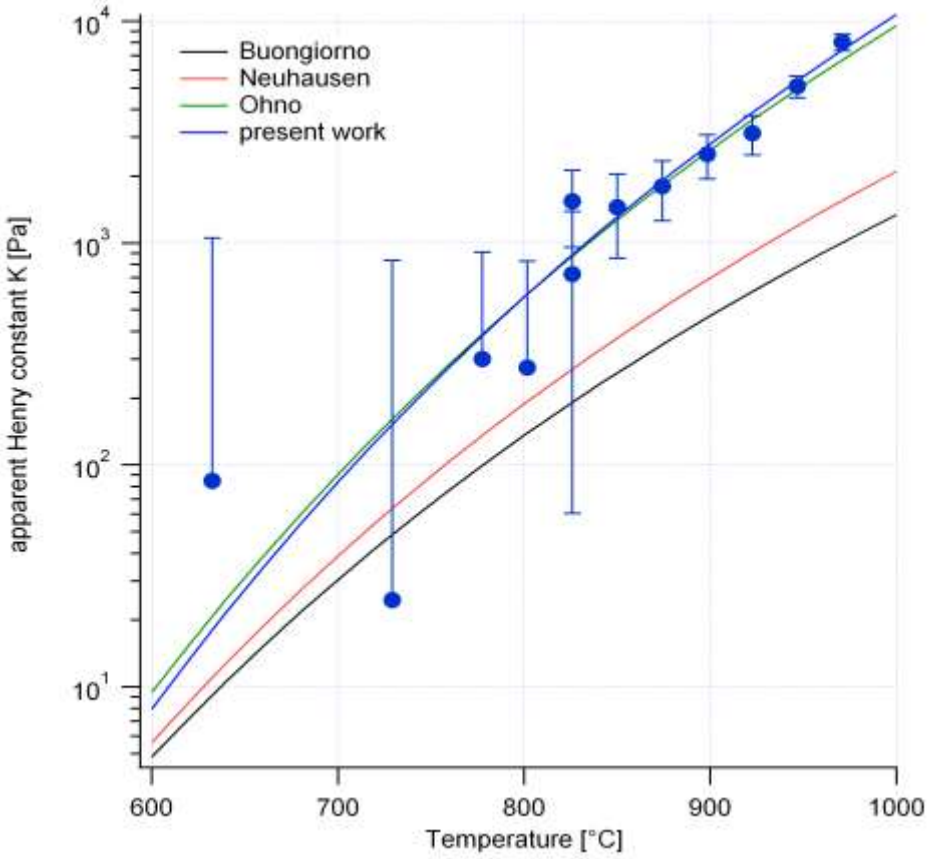

Fig. 15. Henry constants and correlation determined in the present work in comparison with literature data of Po evaporation from LBE.

Our correlation is in good agreement with the correlation of Ohno *et al*. but there is a large gap with the correlations of Neuhausen and Buongiorno *et al*.

The large deviations can occur due to different used setups. For example Buongiorno *et al*. used an autoclave setup with a gas entrainment impeller. Ohno *et al*. placed their quartz boat into a reactor type capsule where the gas flows through to achieve better saturation conditions. It is also sometimes unclear if or how the other groups made their corrections for uncertainties. Especially Buongiorno *et al*. are just pointing out uncertainties for their LSC measurement and electroplating, whereas the other groups take also e.g. the temperature, pressure, self absorption, sample geometry and gas flow rate uncertainties into account and it was pointed out where assumptions for the corrections were made. Our setup is quite similar to the one from Neuhausen *et al*. so there were expected more comparable results then to the other data but the difference could also be caused by the use of a different model for data evaluation. Most important is that it is not sure if the experiments were done under saturated conditions. As this is crucial for the derivation of the Henry constant saturated conditions have to be verified for the present evaporation experiments.

3.4. Flow rate dependence of vapor pressure to locate saturated conditions

For the derivation of the Henry constant saturated vapor is a crucial condition. As it was unknown if the previous experiments were performed under saturated conditions, the gas flow was varied in the experiments and the temperature and experiment time was kept constant (T = 1000 °C; t = 1 h).

For the verification of saturated conditions a plateau region is expected in a diagram of mole fraction of vapor against the flow rate (see Fig. 6). This curve is also expected for a plot of the Henry constant against the flow rate.

The curve of Fig. 6 is simplified; model calculations were done to have an estimate of the saturated region for our experiments. These calculations suggested that the plateau region is very narrow for our experimental setup and conditions [Aerts2012b].

As can be seen on the results (Fig. 16) there is no clear constant region (plateau). The plateau region could be the very narrow region around 40-60 mL/min at STP but it is unsure due to the large scatter of the points and errors. Another possibility is that all experiments were performed in undersaturated conditions. In this case, the plateau region lies at flow rates below 20 mL/min STP. For the former case, limiting diffusion transport should lead to a less steep slope of the curve at low flow rates.

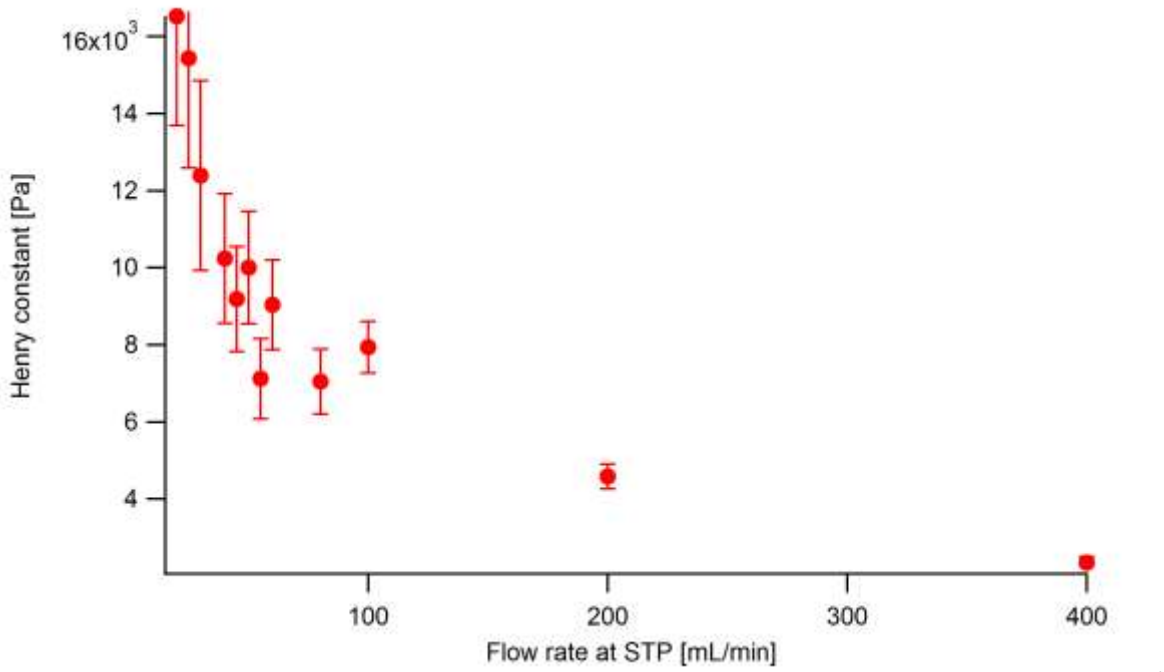

Fig. 16. Experimental derived Henry constant in dependence on flow rate.

3.4.1. Evaporation experiments with insertions

Theoretically it should be possible to reduce the diffusion effect inside the tube during evaporation experiments by adding constrictions before and after the sample. The addition of the insertions inside the tube should, according to model calculations [Aerts2012b], lead to a reduction of the slope in the beginning of the curve. Therefore it is expected to achieve saturated conditions in a larger range of flow rates.

For the experiments insertions with a length of 11 mm and a diameter of 8 mm were added before and behind the quartz boat (Fig. 17. (a)).

The experiments were also performed with a fixed temperature and experiment time (T = 1000 °C; t = 1h) and variation of the flow rate in order to see the influence of the insertions on the Henry constant.

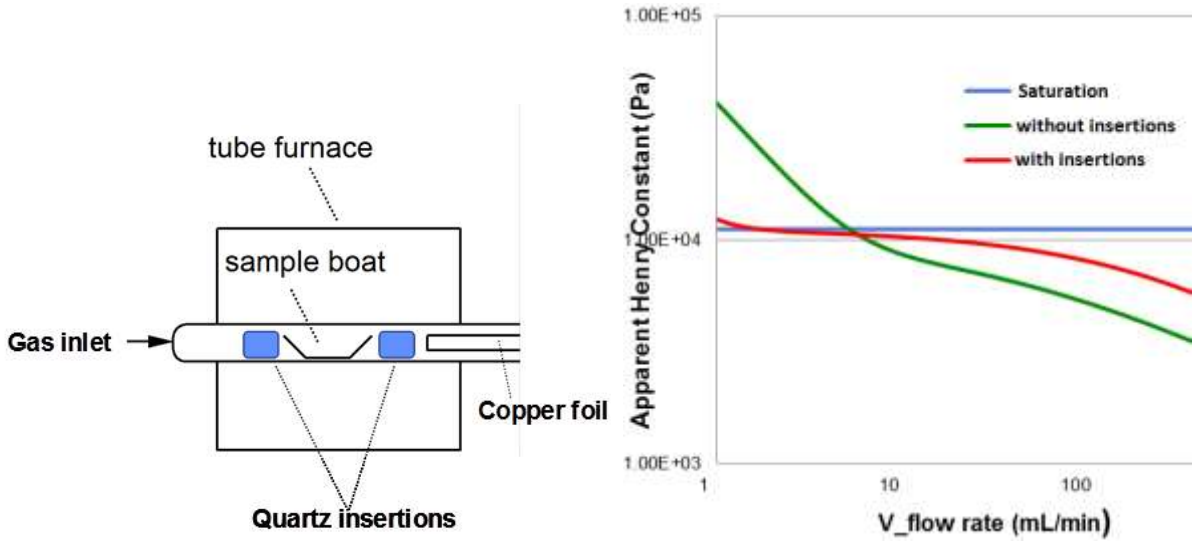

Fig. 17. (a) Scheme of the evaporation tube with insertions **(b)** expected effect of insertions on curve of K versus flow rate.

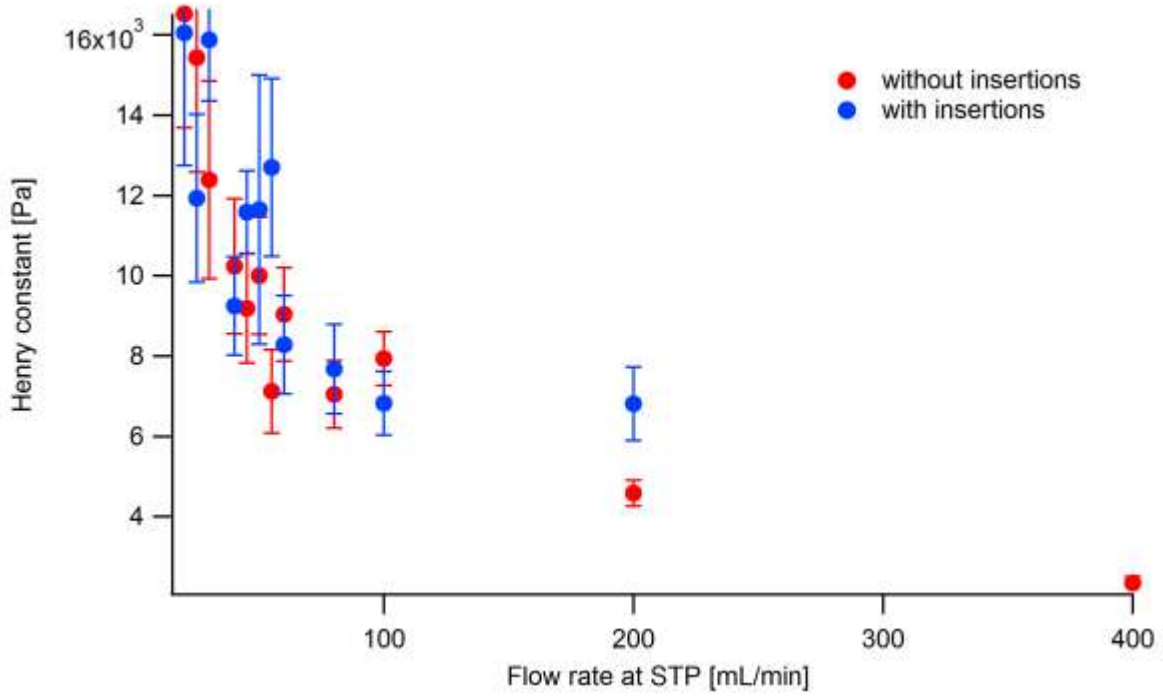

Fig. 18. Comparison of the Henry constant at different flow rates with and without insertions.

The results obtained with insertions show no significant difference compared to the experiments without insertions therefore a plateau region, where saturated conditions are present, is still not found.

The first possibility is that the plateau region is between 40-60 mL/min and the influence of the insertions is not visible due to the large scattering of the measurement points in the expected narrow plateau region. Another possibility is that the insertions have no effect on diffusive transport in our setup. The plateau region can be below 20 mL/min flow rate at STP and the insertions show therefore no effect on the diffusive transport of the vapor. The insertions are also colder than the sample which has been observed due to deposition on the surface of the insertion behind the sample; hence it might be that the insertions show no improvement due to adsorption of Po. The insertions may also disturb the pattern of the gas flow but the exact mechanism is not understood.

Despite the fact that a clear saturated region cannot be observed, our experiments are still in a good agreement with the results of Ohno *et al.* This leads to two assumptions. At first Ohno *et al.* and we worked under saturated conditions but we are not able to verify it as the narrow plateau might be hidden by a large scattering of our data points with large error bars or we both were not able to reach saturated vapor pressure.

3.5. Evaporation of Po in presence of dissolved Pt

Technical LBE, which will be used in MYRRHA, contains many stable impurities already before irradiation [NAA2012]. It has been suggested that even traces of impurities may influence Po evaporation [Aerts2012b]. For example, lanthanides have been proposed to strongly bind Po in solution, thus lowering its vapor pressure [Buongiorno2004]. Based on theoretical calculations of the enthalpy of dissolution and adsorption this also assumed for Po with noble metals like Pt and Pd [OECD2011].

To get a first insight on the influence of noble metals on the evaporation behavior of Po experiments were performed with about 0.1% additional Pt content.

For these experiments the inactive LBE was cut in smaller pieces and flakes and distributed over the whole quartz boat before dilution. Afterwards the active LBE was added and then a platinum wire with a mass of about 2.5 mg was cut in several small piece (around 7-10) and dispersed over the whole quartz boat. Then the sample was homogenized at 600 °C for 30 minutes under a flow of 1 L/min Ar/5% H_2. The LBE concentrates in the middle of the quartz boat due to the surface tension. As the Pt at the ends of the boat disappeared after the homogenization, it is assumed that Pt dissolved in the LBE. After cooling down the sample was cleaned and two samples were cut off for LSC measurement. Afterwards the sample was evaporated at 1000 °C for 1 h at different flow rates of Ar/5% H_2. The results are compared with measurements without Pt in LBE (Fig. 19).

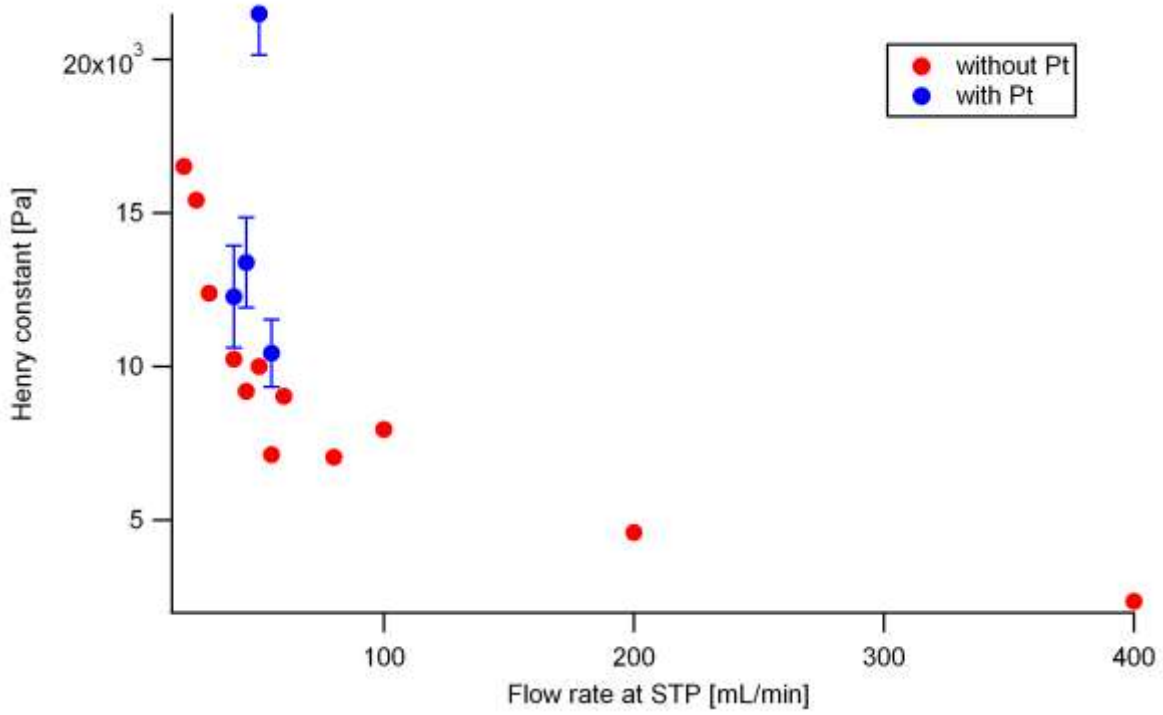

Fig. 19. Henry constants of Po in LBE at different flow rates, without and with addition of 0.1% Pt to LBE.

Three of the four measurements with added Pt to the LBE/Po show a slightly but not significantly higher release compared to the measurements without Pt. It was expected that on the one hand the Po release is hindered by the formation of a platinum-polonium compound as Po shows a high affinity for adsorption on Pt (enthalpy of adsorption = -260.0 kJ/mol) and dissolution in Pt (enthalpy of solution = -21.19 kJ/mol) [OECD2011]. On the other hand it could have been possible to increase the volatility of Po by forming nascent hydrogen with the Pt as a catalyst.

In these experiments Pt is in large excess compared to Po and because Po homogenizes during dilution, it is assumed that an equilibrium between Po and Pt could be established.

It is possible that the equilibrium constant of the possible Pt-Po compound and gaseous Po species is relatively similar to the equilibrium constant of Po evaporating from LBE without Pt. It is also possible that the temperature is too high for the adsorption of Po on Pt and that the interaction between these two is therefore not measureable.

For the possible formation of a volatile H_2Po, where Pt could act as a catalyst, the possibility is very low as the Pt has to react with the hydrogen at the LBE surface together with the Po. Therefore it is possible that the number of formed H_2Po was too low to measure a significant increase of volatile Po species.

4. Conclusion and Outlook

It could be verified that Po distributes homogeneously after dilution which, therefore small samples taken off for LSC measurement can be assumed to be representative for the whole evaporation sample.

The kinetics of Po evaporation from LBE were measured showing an exponential release similar to ideal evaporation behavior. No difference on the evaporation could be measured by using either 100% Ar or Ar/5% H_2.

Evaporation experiments with variation of temperature showed a fractional release similar to Neuhausen *et al.* [Neuhausen2004]. From these experiments an apparent Henry constant correlation was derived showing a good agreement with the correlation from Ohno *et al.* [Ohno2006] which is considered to be the most reliable one [OECD2011].

In experiments with varying flow rate, no obvious plateau region, were saturated conditions are present, could be found. Additional insertions showed no influence on the flow rate dependency. Changes on the setup could improve saturated conditions and therefore might enlarge the possible narrow saturated region.

First experiments with addition of 0.1% Pt, which was suggested to influence the evaporation behavior of Po, showed no significant difference on the evaporation.

5. References

[Abakumov1974] A. S. Abakumov, Z. V. Ershova, *Vapor Tension of Polonium and Lead Polonide*, Radiokhimiya, Vol. 16, pp. 397-401, Soviet Radiochemistry, Vol. 16, pp. 396-399, 1974.

[Abakumov1982] A. S. Abakumov, *Thermal reactions of polonium*, Russ. Chem. Rev. 51, pp. 622-629, 1982.

[Aerts2011a] A. Aerts, *Polonium production, volatilization and release in MYRRHA, Internal Report*, SCK•CEN-I-239, 2011.

[Aerts2011b] A. Aerts, *Determination of Po-210 activity in irradiated LBE by liquid scintillation counting*, SCK•CEN Technical Note, 2011.

[Aerts2012a] A. Aerts, *Determination of solute vapor pressure by the transpiration method: theory*, Version1.1, Internal Report, SCK•CEN-I-xxx, 2012.

[Aerts2012b] A. Aerts, personal communication.

[Bagnall1969] K. W. Bagnall, *The Chemistry of Polonium, Gmelin Handbook of Inorganic and Organometallic Chemistry*, 1969.

[Booth2009] A. M. Booth, T. Markus, G. McFiggans, C. J. Percival, M. R. Mcgillen, and D.O. Topping, *Design and construction of a simple Knudsen Effusion Mass Spectrometer (KEMS) system for vapor pressure measurements of low volatility organics*, Atmos. Meas. Tech., 2, 355–361, 2009.

[BR2] *BR2 reactor* (http://www.sckcen.be/en/Our-Research/Scientific-Institutes-Expert-Groups/Nuclear-Materials-Science/Belgian-Reactor-2).

[Brooks1904] H. Brooks, *A volatile product from radium*, Nature 70, p. 270, 1904.

[Buongiorno2003] J. Buongiorno, C. Larson, K. R. Czerwinski, *Speciation of polonium released from molten lead bismuth*, Radiochim. Acta 91, pp. 153–158, 2003.

[Buongiorno2004] J. Buongiorno, E. P. Loewen, K. R. Czerwinski, C. Larson, *Studies of polonium removal from molten lead-bismuth for lead-alloy-cooled reactor applications*, Nucl. Tech., Vol. 147, pp. 406-417, 2004.

[De Bruyn2011] D. De Bruyn, H..Abderrahim, P. Baeten, R. Fernandez, *MYRRHA, the Multi-purpose Hybrid Research Reactor for High-tech Applications*, Proceedings of ICAPP 2011, Paper 11140, Nice, France, May 2-5, 2011.

[Feuerstein1992] H. Feuerstein, J. Oschinski, S. Horn, *Behavior of Po-210 in molten Pb-17Li*, Proceedings of the Fifth International Conference on Fusion Reactor Materials (ICFRMS-5), J. Nucl. Mat., Vol. 191-194, Part A, pp. 288-291, 1992.

[Fleischer1988] R. L. Fleischer, *Nuclear track studies of alpha-recoil damage in nature: relation to isotopic disequilibrium and leaching of radionuclides*, Int. J. Radiat. Instrum., Part D, Nucl. Tracks Radiat. Meas., Vol. 14, No. 4, pp. 437-446, 1988.

[GIF] US DOE, Nuclear Energy Research Advisory Committee, *A Technology Roadmap for Generation IV Nuclear Energy Systems*, GIF-002-00, 2002.

[Heinitz2010] S. Heinitz, D. Schumann, J. Neuhausen, S. Müller, *Polonium segregation in lead-bismuth eutectic*, 2009 Annual Report, Labor für Radio- und Umweltchemie der Universität Bern und des Paul Scherrer Instituts, p. 59, 2010.

[INL] Idaho National Laboratory, Fact Sheets, 21st Century Science & Technology, http://www.inl.gov/research/lead-cooled-fast-reactor/

[Jolkonnen2009] M. Jolkonnen, *Report on Source Term Assessment for XT-ADS and the lead cooled EFIT*, EUROTRANS, 2009.

[Magill2006] J. Magill, G. Pfennig, J. Galy, *Chart of the Nuclides*, 7th Edition, 2006.

[Merten1967] U. Merten, W. Bell, *The characterization of high-temperature vapors by J.L. Margrave*, p. 91-114, Wiley, New York, 1967.

[Moyer1956] H.V. Moyer (Ed.): *Polonium*. U.S. Atomic Energy Commission Report TID-5221, 1956.

[NAA2012] *Neutron Activation Analysis Report*, Nr. 06-045, SCK•CEN, 2012.

[Neuhausen2003] J. Neuhausen, B. Eichler, *Extension of Miedema's Macroscopic Atom Model to the Elements of Group 16 (O, S, Se, Te, Po)* - PSI Bericht Nr. 03-13, 2003.

[Neuhausen2004] J. Neuhausen, U. Köster, B. Eichler, *Investigation on evaporation characteristics of polonium and its lighter homologues selenium and tellurium from liquid Pb-Bi-eutecticum*, Radiochim. Acta, 92, pp. 917-923, 2004.

[Neuhausen2012] J. Neuhausen, *Volatilization of radionuclides in HLM systems, International workshop on innovative nuclear reactors cooled by heavy liquid metals: Status and perspectives*, Pisa, 17th-20th April, 2012.

[Rizzi2011a] M. Rizzi, S. Lüthi, J. Neuhausen, D. Schumann, *^{206}Po evaporation studies from liquid lead and liquid lead-gold*, 2010 Annual Report, Labor für Radio- und Umweltchemie der Universität Bern und des Paul Scherrer Instituts, p. 41, 2011.

[Rizzi2011b] M. Rizzi, J. Neuhausen, R. Eichler, D. Schumann, *Thermochromatographic investigation of Polonium-206*, 2010 Annual Report, Labor für Radio- und Umweltchemie der Universität Bern und des Paul Scherrer Instituts, p. 42, 2011.

[Trenn1980] T. J. Trenn, *The phenomenon of aggregate recoil: the premature acceptance of an essentially incorrect theory,* Annals of Science, 37: 1, pp. 81 — 100, 1980.

[Ohno2006] S. Ohno, Y. Kurata, S. Miyahara, R. Katsura, S. Yoshida, *Equilibrium Evaporation Behavior of Polonium and Its Homologue Tellurium in Liquid Lead-Bismuth Eutectic*, J. Nucl. Sci. Technol., Vol. 43, No. 11, pp. 1359–1369, 2006.

[OECD2007] A. Terlain, V. Sobolev, J.-L. Courouau, L. Martinelli, P. Agostini, A. Ciampichetti, N. Li, H. Glasbrenner, Handbook on Lead-bismuth Eutectic Alloy and Lead Properties, Materials Compatibility, Thermal-hydraulics and Technologies; Chapter 3 Thermodynamic relationships and chemistry, OECD, 2007.

[OECD2011] J. Neuhausen, A. Aerts, H. Glasbrenner, S. Heinitz, M. Jolkkonen, Y. Kurata, T. Obara, N. Thiollière, L. Zanini, Handbook on Lead-bismuth Eutectic Alloy and Lead Properties, Materials Compatibility, Thermal-hydraulics and Technologies; Chapter 5: Properties of Irradiated LBE and Pb, OECD, 2011.

[Zrodnikov1999] A.V. Zrodnikov, V.I. Chitakin, B.F. Gromov, O.G. Grigoryv, A.V. Dedoul, G.I. Toshinsky, YU.G. Dragunov, V.S. Stepanov, *Use of Russian technology of ship reactors with lead-bismuth as coolant in nuclear power*, Proc. Int. Conf. Future Nuclear Systems (Global `99), Jackson Hole, Wyoming, 1999.

6. Appendices

6.1. Production of Po-210/LBE

The content of Po-210 and Bi-210 in the sample is given by following set of differential equations:

$$dN_{Bi\text{-}210}/dt = k - \lambda_{Bi\text{-}210} * N_{Bi\text{-}210} \quad \text{(Eq. A1)}$$

$$\frac{dN_{Po\text{-}210}}{dt} = N_{Bi\text{-}210} * \lambda_{Bi\text{-}210} - N_{Po\text{-}210} * \lambda_{Po\text{-}210} \quad \text{(Eq. A2)}$$

N_x = number of atoms of nuclide *x*

k = Production rate (s^{-1})

λ_x = decay constant of of nuclide *x* (s^{-1})

The term $N_{Bi} * \lambda_{Bi}$ describes the Po-210 formation due to the decay of Bi-210 and the term $N_{Po} * \lambda_{Po}$ describes the decay of the Po-210 itself.

Therefore the Po-210 formation due to the decay of Bi-210 can be derived by integration of Eq. A2 which leads to a Bateman equation:

$$N_{Po\text{-}210}(t) = \left[\frac{\lambda_{Bi\text{-}210}}{\lambda_{Po\text{-}210} - \lambda_{Bi\text{-}210}} \right] * N_{Bi\text{-}210}(0) * [\exp(-\lambda_{Bi\text{-}210} * t) - \exp(-\lambda_{Po\text{-}210} * t)] \quad \text{(Eq. A3)}$$

The equation describes the variation of the number of daughter nucleii with variation of time as consequence of the formation and subsequent decay. The last term takes into account the decay of already present Po-210 which can be important for other systems with different nuclides. As there is usually no Po-210 present or to a negligible amount the last term can be canceled out.

By integration of Eq. A1 one gains:

$$N_{Bi\text{-}210}(0) = \frac{k}{\lambda_{Bi\text{-}210}} * (1 - \exp(-\lambda_{Bi\text{-}210} * t_{irr})) \quad \text{(Eq. A4)}$$

t_{irr} = irradiation time [s]

The production rate k for the irradiation in a reactor depends on the number of target nucleii, the cross section and the neutron flux: (t)

$$k = \Phi * N_x * \sigma_x \quad \text{(Eq. A5)}$$

σ_x = neutron capture cross section of the concerning nuclide [b = 10^{-24} cm²]

Φ = neutron flux [cm^{-2} s^{-1}]

As Bi-209 is the target nuclide for the generation of Bi-210 which then decays to Po-210, the formation of the Bi-210 in a reactor is described by following activation equation after inserting the production rate Eq. A5 into Eq. A4:

$$N_{Bi\text{-}210}(0) = \frac{N_{Bi\text{-}209} * \sigma_{Bi\text{-}209} * \Phi * (1 - \exp(-\lambda_{Bi\text{-}210} * t_{irr}))}{\lambda_{Bi\text{-}210}} \quad \text{(Eq. A6)}$$

The Po-210 is generated by the decay of the Bi-210. Due to the shorter half-life of the mother nuclide Bi-210 no equilibrium conditions are present in the system.

Inserting the activation equation Eq. A6 into Eq. A3 one finally arrives at:

$$N_{Po\text{-}210}(t) = \left[\frac{\lambda_{Bi\text{-}210}}{\lambda_{Po\text{-}210} - \lambda_{Bi\text{-}210}} \right] * \frac{N_{Bi\text{-}209} * \sigma_{Bi\text{-}209} * \Phi * (1 - \exp(-\lambda_{Bi\text{-}210} * t_{irr}))}{\lambda_{Bi\text{-}210}} * [\exp(-\lambda_{Bi\text{-}210} * t) - \exp(-\lambda_{Po\text{-}210} * t)] \quad \text{(Eq. A7)}$$

The maximal possible Po content after irradiation can be calculated as follows:

$$\lambda_{Bi\text{-}210} * \exp(-\lambda_{Bi\text{-}210} * t) = \lambda_{Po\text{-}210} * \exp(-\lambda_{Po\text{-}210} * t) \quad \text{(Eq. A8)}$$

Yielding the maximal $N_{Po\text{-}210\text{-}max}$ with:

$$t_{max} = \frac{\ln (\lambda_{Po\text{-}210}/\lambda_{Bi\text{-}210})}{(\lambda_{Po\text{-}210}-\lambda_{Bi\text{-}210})} \qquad \text{(Eq. A9)}$$

Inserting the decay constants $\lambda_{Po\text{-}210} = 0.00501\ d^{-1}$ and $\lambda_{Bi\text{-}210} = 0.13827\ d^{-1}$ one obtains that the maximal Po-210 content is reached after $t_{max} = 24.9$d of letting Bi-210 decay.

6.2. List of Tables

6.3. List of Figures

6.4. Abbreviations

ADS	Accelerator Driven System
GenIV	Generation IV
LBE	Lead-bismuth eutectic
LFR	Lead fast reactor
LSC	Liquid scintillation counting
MAC	Maximal allowed concentration
MYRRHA	Multi hYbrid Research reactor for High-tech application
SCK•CEN	Belgian Nuclear Research Center
STP	Standard temperature and pressure

7. Data

7.1. Homogeneity of Po/LBE samples after dilution

Sample	gross CPM	net CPM	SIS FLAG	gross CPS	net CPS	sample mass (g)	Bq/g
BG	55	0	233,27	0,9	0,0	0,099	0,0
HOM1	3373	3318	404,37	56,2	55,3	0,113	488,1
HOM2	3474	3419	389,27	57,9	57,0	0,116	491,6
HOM3	3365	3310	384,54	56,1	55,2	0,112	492,6
HOM4	3126	3071	380,49	52,1	51,2	0,103	499,3
HOM5	2822	2767	384,49	47,0	46,1	0,095	484,9
HOM6	3092	3037	382,59	51,5	50,6	0,112	452,3
HOM7	3263	3208	380,58	54,4	53,5	0,111	482,2
HOM8	2696	2641	380,77	44,9	44,0	0,100	438,9
HOM9	4005	3950	390,06	66,7	65,8	0,137	481,9
HOM10	3249	3194	381,22	54,2	53,2	0,110	483,1

7.2. Kinetics of Polonium evaporation

7.2.1. 100% Ar

	CPS	Bq	m_LBE (g)	Bq/g	error_Bq/g	ΔBq/g	error ΔBq/g
BG	0,92						
Before evap 1	7,135	6,78	0,0279				
Before evap 2	8,542	8,92	0,0342	253,10	25,71		
Evap to 2 min	7,126	6,77	0,0278	243,38	34,76	9,72	43,23
Evap to 5 min	5,767	5,00	0,0225	222,02	31,80	31,08	40,89
Evap to 9 min	7,167	6,96	0,0298	233,73	33,36	19,36	42,11
Evap to 15 min	6,769	6,60	0,0309	213,60	30,47	39,50	39,87
Evap to 23 min	5,754	5,46	0,0309	176,30	25,16	76,80	35,97
background	0,932						
Evap to 30 min	4,664	4,08	0,0277	147,03	21,01	106,07	33,20
Evap to 37.5 min	1,616	0,78	0,0307	25,53	3,66	227,57	25,97
Evap to 45 min	2,979	2,13	0,0228	93,52	13,41	159,58	29,00
Evap to 52.5 min	2,823	2,02	0,0255	79,51	11,38	173,59	28,12
Evap to 60 min	2,535	1,74	0,0268	65,05	9,31	188,05	27,34

	% release total	error_ %release	Time (min)	total time (min)	ΔBq/g differential	% release differental
Before evap 1						
Before evap 2						
Evap to 2 min	3,84	17,09	2,0	2	9,72	3,84
Evap to 5 min	12,28	16,20	3,0	5	21,37	8,78
Evap to 9 min	7,65	16,66	4,0	9	-11,72	-5,28
Evap to 15 min	15,60	15,83	6,0	15	20,13	8,61
Evap to 23 min	30,34	14,54	8,0	23	37,30	17,46
background						0,00
Evap to 30 min	41,91	13,79	7,0	30	29,28	16,61
Evap to 37.5 min	89,91	13,74	7,5	38	121,50	82,64
Evap to 45 min	63,05	13,13	7,5	45	-67,99	-266,34
Evap to 52.5 min	68,59	13,11	7,5	53	14,01	14,98
Evap to 60 min	74,30	13,18	7,5	60	14,46	18,18

7.2.2. Ar/5% H_2

	CPS	Bq	m_LBE (g)	Bq/g	error_Bq/g	ΔBq/g	error_ΔBq/g
BG	0,92						
Before evap 1	6,513	6,12	0,0282				
Before evap 2	6,76	6,37	0,0279	222,97	22,52		
Evap to 2 min	6,45	6,15	0,0296	207,84	29,66	15,13	37,24
Evap to 5 min	6,123	5,76	0,0292	197,13	28,14	25,84	36,04
Evap to 9 min	4,806	4,26	0,0283	150,57	21,51	72,40	31,14
Evap to 15 min	5,395	4,65	0,0233	199,95	28,62	23,01	36,42
Evap to 23 min	5,266	4,85	0,0299	162,08	23,14	60,89	32,28
Evap to 30 min	3,629	3,20	0,0350	91,55	13,06	131,42	26,03
Evap to 37.5 min	3,634	2,91	0,0262	111,12	15,89	111,85	27,56
Evap to 45 min	3,071	2,42	0,0308	78,66	11,24	144,31	25,16
Evap to 52.5 min	2,661	1,96	0,0305	64,06	9,16	158,90	24,31
Evap to 60 min	2,247	1,51	0,0314	47,91	6,85	175,06	23,54

	% release total	error_ %release	Time (min)	total time (min)	ΔBq/g differential	% release differental
Before evap 1						
Before evap 2						
Evap to 2 min	6,79	16,72	2,0	2	15,13	6,79
Evap to 5 min	11,59	16,21	3,0	5	10,71	5,15
Evap to 9 min	32,47	14,34	4,0	9	46,56	23,62
Evap to 15 min	10,32	16,37	6,0	15	-49,38	-32,80
Evap to 23 min	27,31	14,74	8,0	23	37,88	18,94
Evap to 30 min	58,94	13,10	7,0	30	108,41	54,22
Evap to 37.5 min	50,16	13,36	7,5	38	-19,57	-21,38
Evap to 45 min	64,72	13,04	7,5	45	32,46	29,21
Evap to 52.5 min	71,27	13,06	7,5	53	14,59	18,55
Evap to 60 min	78,51	13,20	7,5	60	16,16	25,22

7.2.3. Ar/5% H_2 with 3 minutes preheating

	CPS	Bq	m_LBE (g)	Bq/g	error_Bq/g	ΔBq/g	error_ΔBq/g
BG	0,931						
Before evap 1	12,72	12,92	0,0282				
Before evap 2	12,88	13,46	0,0307	448,30	32,02		
Evap to 2 min	10,24	10,52	0,0310	339,42	34,25	108,88	46,88
Evap to 5 min	12,87	14,01	0,0343	408,49	41,18	39,82	52,16
Evap to 9 min	9,345	9,12	0,0272	335,75	33,92	112,55	46,65
Evap to 15 min	9,845	10,34	0,0333	310,73	31,34	137,57	44,80
Evap to 23 min	6,215	5,59	0,0247	225,81	22,85	222,49	39,34
Evap to 30 min	5,823	5,35	0,0279	191,87	19,40	256,43	37,44
Evap to 37.5 min	5,313	4,97	0,0311	159,76	16,14	288,54	35,86
Evap to 45 min	4,809	4,54	0,0339	134,01	13,53	314,29	34,76
Evap to 52.5 min	3,311	2,69	0,0305	87,97	8,90	360,33	33,23
Evap to 60 min	2,959	2,20	0,0269	81,94	8,31	366,36	33,08

	% release total	error_ %release	Time (min)	total time (min)	ΔBq/g differential	% release differental
Before evap 1						
Before evap 2						
Evap to 2 min	24,29	10,60	2,0	2	108,88	24,29
Evap to 5 min	8,88	11,65	3,0	5	-69,07	-20,35
Evap to 9 min	25,11	10,56	4,0	9	72,74	17,81
Evap to 15 min	30,69	10,23	6,0	15	25,02	7,45
Evap to 23 min	49,63	9,46	8,0	23	84,92	27,33
Evap to 30 min	57,20	9,30	7,0	30	118,86	38,25
Evap to 37.5 min	64,36	9,23	7,5	38	32,11	16,74
Evap to 45 min	70,11	9,23	7,5	45	25,75	16,12
Evap to 52.5 min	80,38	9,38	7,5	53	46,04	34,36
Evap to 60 min	81,72	9,41	7,5	60	6,03	6,85

7.3. Temperature dependence of Po vapor pressure

		T (°C)	CPS net	m LBE (g)	CPS/g	error CPS/g	ΔCPS net	Error ΔCPS net	release (%)	error of release (%)
BG										
1	before	650	11,16	0,0325	343,28	48,94				
2	after	650	9,77	0,0289	337,51	48,17	5,78	68,67	1,68	20,00
3	before	750	10,09	0,0302	334,36	47,70				
4	after	750	9,86	0,0297	332,60	47,46	1,76	67,28	0,53	20,12
5	before	850		0,0289						
6	before	850	11,02	0,0338	351,23	35,69				
7	after	850	9,54	0,0327	291,36	41,54	59,87	54,76	17,05	15,69
8	before	950		0,0327						
9	before	950	10,68	0,0286	348,09	35,24				
10	after	950	4,78	0,0321	148,96	21,25	199,13	41,15	57,21	13,16
BG										
12	before	900		0,0264						
13	before	900	5,23	0,0251	203,42	20,57				
14	after	900		0,0322						
15	after	900	3,99	0,0304	127,45	12,87	75,97	24,27	37,35	12,51
16	before	925		0,0232						
17	before	925	4,48	0,0259	182,48	18,47				
18	after	925		0,0350						
19	after	925	3,12	0,0290	97,52	10,00	84,96	21,01	46,56	12,44
BG										
21	before	1000		0,0312						
22	before	1000	8,51	0,0376	247,63	23,40				
23	after	1000		0,0328						
24	after	1000	1,54	0,0321	47,57	5,08	200,06	23,95	80,79	12,32
BG										
26	before	975		0,0361						
27	before	975	6,59	0,0300	199,61	20,29				
28	after	975		0,0364						
29	after	975	2,15	0,0388	57,06	5,76	142,55	21,10	71,42	12,82
30	before	800		0,0273						
31	before	800	6,09	0,0263	227,24	22,97				
32	after	800		0,0330						
33	after	800	7,05	0,0335	212,12	21,39	15,12	31,39	6,66	13,83
34	before	825		0,0302						
35	before	825	6,22	0,0311	203,04	20,52				
36	after	825		0,0319						
37	after	825	6,17	0,0332	189,61	19,13	13,43	28,06	6,61	13,83
38	before	850		0,0349						
39	before	850	7,01	0,0286	220,74	22,44				
40	after	850		0,0246						
41	after	850	3,96	0,0276	151,90	15,40	68,83	27,21	31,18	12,73
42	before	875		0,0343						
43	before	875	7,85	0,0286	249,39	25,32				
44	after	875		0,0349						
45	after	875	5,83	0,0310	176,77	17,87	72,62	30,99	29,12	12,77

T (°C)	T (K)	Vflow corrected (m3/s)	m(t=0) (g)	delta m	m(t=60min) (g)
650	923	5,063E-06	2,42	0,00	2,42
750	1023	5,603E-06	2,03	0,00	2,03
850	1123	6,144E-06	1,91	0,01	1,91
950	1223	6,684E-06	1,85	0,03	1,81
900	1173	6,414E-06	1,92	0,02	1,90
925	1198	6,549E-06	2,00	0,03	1,97
1000	1273	6,954E-06	2,46	0,09	2,37
975	1248	6,819E-06	2,05	0,06	1,99
800	1073	5,873E-06	2,15	0,00	2,15
825	1098	6,009E-06	1,96	0,00	1,96
850	1123	6,144E-06	2,06	0,01	2,05
875	1148	6,279E-06	2,10	0,01	2,09

T (°C)	n(0)	p LBE/Po (Pa)	<ln(n(t)/n(0))>	K (Pa)	abs. error_K (Pa)
650	0,012	0,26	-0,018	84,768	-969,695
750	0,010	2,95	-0,006	24,587	-811,123
850	0,009	21,67	-0,191	723,006	-662,615
950	0,009	114,51	-0,867	3124,779	-630,702
900	0,009	51,64	-0,477	1800,580	-539,516
925	0,010	77,55	-0,640	2516,965	-566,498
1000	0,012	238,29	-1,689	8046,902	-679,650
975	0,010	166,42	-1,280	5092,635	-570,087
800	0,010	8,38	-0,070	299,931	-608,231
825	0,009	13,62	-0,071	274,176	-554,020
850	0,010	21,67	-0,378	1539,030	-584,750
875	0,010	33,78	-0,350	1448,681	-593,467

7.4. Flow rate dependence of vapor pressure to locate saturated conditions

	before/after evap	V_flow(mL/min)	V_flow(m3/s)	CPS	Bq	avg Bq
1	BG			0,86		
2	before	0	0,00E+00	6,56	6,24	
3	before	0	0,00E+00	7,10	6,56	6,40
4	after	0	0,00E+00	8,93	8,46	
5	after	0	0,00E+00	6,47	6,67	7,56
6	before	20	3,33E-07	8,53	8,04	
7	before	20	3,33E-07	9,26	9,66	8,85
8	after	20	3,33E-07	6,79	6,91	
9	after	20	3,33E-07	5,41	5,63	6,27
10	before	40	6,67E-07	6,93	6,71	
11	before	40	6,67E-07	7,20	6,83	6,77
12	after	40	6,67E-07	3,46	2,77	
13	after	40	6,67E-07	3,80	3,10	2,94
14	before	60	1,00E-06	10,55	10,62	
15	before	60	1,00E-06	7,33	8,05	9,34
16	after	60	1,00E-06	3,24	2,53	
17	after	60	1,00E-06	3,42	2,73	2,63
18	before	80	1,33E-06	9,06	8,98	
19	before	80	1,33E-06	7,36	7,67	8,33
20	after	80	1,33E-06	3,33	2,74	
21	after	80	1,33E-06	2,93	2,48	2,61
22	BG			1,33		
23	before	100	1,67E-06	8,42	7,76	
24	before	100	1,67E-06	9,52	9,27	8,51
25	after	100	1,67E-06	2,89	1,90	
26	after	100	1,67E-06	2,36	1,18	1,54
27	before	200	3,33E-06	8,02	7,65	
28	before	200	3,33E-06	8,26	7,88	7,76
29	after	200	3,33E-06	2,31	1,10	
30	after	200	3,33E-06	2,46	1,30	1,20
31	before	400	6,67E-06	10,19	10,52	
32	before	400	6,67E-06	8,94	8,75	9,63
33	after	400	6,67E-06	2,47	1,26	
34	after	400	6,67E-06	2,53	1,43	1,34
35	before	30	5,00E-07	8,06	7,78	
36	before	30	5,00E-07	7,71	6,94	7,36
37	after	30	5,00E-07	5,05	4,01	
38	after	30	5,00E-07	5,74	4,99	4,50
39	before	50	8,33E-07	7,16	6,98	
40	before	50	8,33E-07	9,73	8,90	7,94
41	after	50	8,33E-07	3,90	3,07	
42	after	50	8,33E-07	4,39	3,42	3,25
43	before	25	4,17E-07	8,26	8,24	
44	before	25	4,17E-07	9,44	8,94	8,59
45	after	25	4,17E-07	3,96	3,08	

46	after	25	4,17E-07	5,07	3,99	3,53
47	BG			1,38		
48	before	45	7,50E-07	6,06	5,07	
49	before	45	7,50E-07	7,29	6,74	5,90
50	after	45	7,50E-07	3,30	2,13	
51	after	45	7,50E-07	3,56	2,51	2,32
52	before	55	9,17E-07	6,10	5,70	
53	before	55	9,17E-07	4,42	3,21	4,45
54	after	55	9,17E-07	2,87	1,72	
55	after	55	9,17E-07	2,86	1,69	1,71
56	before	20	3,33E-07	4,35	3,47	
57	before	20	3,33E-07	4,34	3,45	3,46
58	after	20	3,33E-07	2,95	1,89	
59	after	20	3,33E-07	2,35	1,15	1,52

	m_LBE (g)	avg m_LBE (g)	Bq/g	error Bq/g	ΔBq/g	% release	error %release
1	0,028						
2	0,024						
3	0,024	0,024	264,232	27,897			
4	0,036						
5	0,024	0,030	253,490	25,886	10,741	4,065	14,409
6	0,033						
7	0,034	0,033	267,371	25,320			
8	0,039						
9	0,029	0,034	184,602	19,304	82,769	30,957	12,264
10	0,027						
11	0,025	0,026	259,293	27,111			
12	0,025						
13	0,028	0,027	110,426	10,888	148,867	57,413	12,767
14	0,039						
15	0,025	0,032	289,908	30,276			
16	0,026						
17	0,028	0,027	97,355	9,587	192,552	66,419	12,966
18	0,035						
19	0,029	0,032	259,568	26,077			
20	0,036						
21	0,029	0,033	80,273	8,157	179,295	69,074	12,608
22	0,028						
23	0,031						
24	0,038	0,034	247,631	23,402			
25	0,033						
26	0,032	0,032	47,569	5,082	200,062	80,790	12,321
27	0,032						
28	0,031	0,031	247,179	25,105			
29	0,032						
30	0,035	0,034	35,516	3,493	211,664	85,632	13,446
31	0,033						
32	0,029	0,031	312,423	33,222			
33	0,036						
34	0,033	0,035	38,923	3,838	273,500	87,542	14,186
35	0,028						

36	0,027	0,027	269,952	28,934			
37	0,031						
38	0,036	0,034	133,369	12,624	136,583	50,595	12,890
39	0,025						
40	0,036	0,031	260,205	26,641			
41	0,030						
42	0,036	0,033	98,956	10,037	161,250	61,970	12,647
43	0,029						
44	0,034	0,032	272,613	27,866			
45	0,026						
46	0,031	0,028	125,045	13,127	147,568	54,131	12,581
47							
48	0,026						
49	0,031	0,029	205,219	20,857			
50	0,027						
51	0,031	0,029	79,921	8,097	125,298	61,056	12,544
52	0,036						
53	0,023	0,030	150,538	15,655			
54	0,030						
55	0,030	0,030	56,884	5,753	93,654	62,213	12,830
56	0,033						
57	0,032	0,032	106,624	10,760			
58	0,034						
59	0,031	0,033	46,639	4,785	59,986	56,259	12,418

V_flow (ml/min)	V_flow(m3/s)	V_flow corrected (m3/s)	m(t=0) (g)	delta m	m (t=60min) (g)
20	3,33E-07	1,42E-06	2,60	0,0287	2,5723
40	6,67E-07	2,85E-06	2,40	0,0514	2,3445
60	1,00E-06	4,27E-06	2,50	0,0673	2,4316
80	1,33E-06	5,69E-06	2,43	0,0756	2,3568
100	1,67E-06	7,12E-06	2,46	0,094	2,3692
200	3,33E-06	1,42E-05	2,50	0,1308	2,3741
400	6,67E-06	2,85E-05	2,61	0,124	2,481
30	5,00E-07	2,14E-06	2,63	0,0424	2,5839
50	8,33E-07	3,56E-06	2,59	0,0601	2,5313
25	4,17E-07	1,78E-06	2,47	0,0364	2,4354
45	7,50E-07	3,20E-06	2,20	0,0527	2,1438
55	9,17E-07	3,91E-06	2,04	0,0437	1,9919
20	3,33E-07	1,42E-06	2,00	0,0286	1,9703

V_flow (ml/min)	n(0)	P sat	ln(n(t)/n(0))	K (Pa)	error_K (Pa)
20	0,012493	360,4083466	-0,38153	9772,009	-3613,444934
40	0,011508	360,4083466	-0,8753	10239,76	-1681,269207
60	0,012002	360,4083466	-1,1185	9036,038	-1159,607392
80	0,011683	360,4083466	-1,20515	7048,095	-835,6924645
100	0,011831	360,4083466	-1,68867	7941,587	-670,7548061
200	0,012031	360,4083466	-1,99377	4583,916	-325,0356739
400	0,012512	360,4083466	-2,13155	2348,193	-159,7505338
30	0,012614	360,4083466	-0,7214	12395,14	-2456,964023
50	0,012446	360,4083466	-0,99026	9999,672	-1455,295284
25	0,011872	360,4083466	-0,79422	15430,76	-2846,804138
45	0,01055	360,4083466	-0,96732	9189,144	-1363,229096
55	0,009777	360,4083466	-0,99491	7122,335	-1038,488019
20	0,009601	360,4083466	-0,84129	16524,42	-2826,673826

7.4.1. Evaporation experiments with insertions

	before/after	V_flow (mL/min)	CPS	Bq	Avg Bq	m_LBE (g)	Avg m_LBE (g)
1	background		1,38			0,0282	
2	before	20	4,29	2,77		0,0135	
3	before	20	5,12	3,62	3,19	0,0151	0,0143
4	after	20	3,52	2,14		0,0183	
5	after	20	3,45	2,07	2,10	0,0183	0,0183
6	before	30	4,23	2,76		0,0152	
7	before	30	3,95	2,46	2,61	0,0143	0,0147
8	after	30	2,52	1,10		0,0148	
9	after	30	2,34	0,96	1,03	0,0182	0,0165
10	before	40	5,01	3,45		0,0134	
11	before	40	6,53	5,19	4,32	0,0191	0,0162
12	after	40	2,81	1,39		0,0152	
13	after	40	2,81	1,38	1,38	0,0145	0,0149
14	before	50	5,89	4,52		0,0186	
15	before	50	5,92	4,53	4,52	0,0183	0,0184
16	after	50	2,45	1,03		0,0150	
17	after	50	2,32	0,90	0,97	0,0139	0,0144
18	before	60	3,99	2,47		0,0130	
19	before	60	3,80	2,26	2,36	0,0116	0,0123
20	after	60	1,74	0,36		0,0164	
21	after	60	2,14	0,74	0,55	0,0155	0,0160
22	background		0,87			0,0282	
23	before	25	7,23	7,44		0,0324	
24	before	25	6,90	7,15	7,30	0,0335	0,0330
25	after	25	3,84	3,48		0,0325	
26	after	25	4,42	4,22	3,85	0,0337	0,0331
27	before	35	6,60	6,13		0,0247	
28	before	35	7,22	7,01	6,57	0,0275	0,0261
29	after	35	4,30	3,97		0,0314	
30	after	35	4,21	4,08	4,02	0,0357	0,0335
31	before	70	8,98	9,16		0,0294	
32	before	70	11,25	12,80	10,98	0,0365	0,0330
33	after	70	3,86	3,46		0,0315	
34	after	70	3,47	3,07	3,26	0,0332	0,0323
35	before	80	11,74	13,63		0,0379	
36	before	80	8,45	8,43	11,03	0,0281	0,0330
37	after	80	2,63	1,88		0,0244	
38	after	80	3,81	3,48	2,68	0,0334	0,0289
39	before	90	7,75	8,11		0,0330	
40	before	90	8,02	8,63	8,37	0,0349	0,0339
41	after	90	2,43	1,65		0,0235	
42	after	90	2,43	1,96	1,81	0,0378	0,0307
43	before	100	8,36	9,04		0,0348	
44	before	100	7,65	7,58	8,31	0,0286	0,0317
45	after	100	2,29	1,71		0,0344	
46	after	100	2,33	1,74	1,73	0,0342	0,0343

	avg Bq/g	ΔBq/g	Error ΔBq/g	% release	error_%release
1					
2					
3	223,08				
4					
5	114,72	108,37	24,81	48,58	12,11
6					
7	177,26				
8					
9	62,63	114,64	18,55	64,67	12,26
10					
11	265,97				
12					
13	93,11	172,86	28,16	64,99	12,43
14					
15	245,33				
16					
17	66,86	178,47	25,01	72,75	12,45
18					
19	192,46				
20					
21	34,52	157,94	19,35	82,06	12,92
22					
23					
24	221,32				
25					
26	116,49	104,83	32,37	47,37	15,84
27					
28	252,00				
29					
30	119,99	132,02	36,13	52,39	15,87
31					
32	332,78				
33					
34	100,88	231,89	44,28	69,68	15,99
35					
36	334,26				
37					
38	92,75	241,51	50,06	72,25	18,32
39					
40	246,68				
41					
42	58,89	187,79	31,34	76,13	15,83
43					
44	262,14				
45					
46	50,29	211,85	44,15	80,82	21,52

V_flow(mL/min)	v_flow correction (m3/s)	m(t=0) (g)	delta m	mt (g)	n(0)
20	1,42E-06	2,408	0,0300	2,378	0,0116
30	2,14E-06	2,296	0,0430	2,253	0,0110
40	2,85E-06	2,215	0,0512	2,163	0,0106
50	3,56E-06	2,259	0,0605	2,199	0,0109
60	4,27E-06	2,255	0,0652	2,189	0,0108
25	1,78E-06	2,309	0,0380	2,271	0,0111
35	2,49E-06	2,175	0,0421	2,133	0,0104
70	4,98E-06	2,453	0,0743	2,379	0,0118
80	5,69E-06	2,432	0,0737	2,358	0,0117
90	6,41E-06	2,192	0,0791	2,113	0,0105
100	7,12E-06	2,126	0,0813	2,045	0,0102

V_flow(mL/min)	Sum i*pi	<ln(n(t)/n(0))>	K (Pa)	s_K (Pa)
20	360,408	-0,68	16059,31	-3308,62
30	360,408	-1,06	15885,34	-2096,54
40	360,408	-1,07	11587,19	-1517,96
50	360,408	-1,33	11653,44	-1224,93
60	360,408	-1,75	12706,44	-1032,47
25	360,408	-0,66	11939,07	-3347,38
35	360,408	-0,76	9247,10	-2216,02
70	360,408	-1,22	8287,32	-1220,85
80	360,408	-1,31	7674,78	-1108,56
90	360,408	-1,47	6829,26	-787,19
100	360,408	-1,69	6817,54	-914,68

7.5. Evaporation of Po in presence of dissolved Pt

	V_flow(mL/min)	V_flow(m3/s)	CPS	Bq	avg_Bq	m_LBE (g)
BG			1,38			0,028
Before	50	8,33E-07	3,84	0,28		0,029
Before	50	8,33E-07	4,35	0,33	3,01	0,029
After	50	8,33E-07	1,62	0,03		0,031
After	50	8,33E-07	1,63	0,03	0,27	0,026
BG			0,91			
Before	40	6,67E-07	6,54	0,68		0,036
Before	40	6,67E-07	3,58	0,29	4,78	0,025
After	40	6,67E-07	1,69	0,08		0,026
After	40	6,67E-07	2,79	0,21	1,46	0,030
Before	45	7,50E-07	6,93	0,66		0,028
Before	45	7,50E-07	6,04	0,55	6,00	0,025
After	45	7,50E-07	2,58	0,18		0,026
After	45	7,50E-07	2,26	0,15	1,61	0,026
Before	55	9,17E-07	5,07	0,47		0,030
Before	55	9,17E-07	5,28	0,48	4,71	0,028
After	55	9,17E-07	2,15	0,15		0,033
After	55	9,17E-07	2,07	0,13	1,37	0,030

	V_flow (mL/min)	Avg m_LBE (g)	Bq/g	ΔBq/g	error_ΔBq/g	% release	error_%release
BG							
Before	50						
Before	50	0,03	103,33				
After	50						
After	50	0,03	10,47	92,86	10,52	89,87	13,65
BG							
Before	40						
Before	40	0,03	157,17				
After	40						
After	40	0,03	52,93	104,24	17,56	66,32	13,20
Before	45						
Before	45	0,03	227,83				
After	45						
After	45	0,03	62,66	165,17	23,95	72,50	12,83
Before	55						
Before	55	0,03	162,02				
After	55						
After	55	0,03	43,12	118,90	16,93	73,39	12,81

V_flow(mL/min)	V_flow(m3/s)	V_flow_corrected (m3/s)	m(t=0) (g)	delta m	m (t=60) (g)
50	8,33E-07	3,56E-06	2,3831	0,0671	2,316
40	6,67E-07	2,85E-06	2,2661	0,0506	2,2155
45	7,50E-07	3,20E-06	2,3516	0,0555	2,2961
55	9,17E-07	3,91E-06	2,19	0,0637	2,1263

V_flow(mL/min)	n(0)	p LBE/Po (Pa)	ln(n(t)/n(0))	K (Pa)	error_K (Pa)
50	0,0114	360,41	-2,32	21492,48	-1338,49
40	0,0109	360,41	-1,11	12280,52	-1655,86
45	0,0113	360,41	-1,31	13389,20	-1461,30
55	0,0105	360,41	-1,35	10442,02	-1103,51

Acknowledgement

I would like to thank Joris van den Bosch for the opportunity to perform my master thesis in his group.

I am deeply indebted to Alexander Aerts. Thank you for the many discussions, the interesting topic, for reviewing my thesis. Thank you for your guidance during the thesis and all your patience.

Muchas gracias to Borja Gonzalez for the introduction of the lab procedures and data analysis and answering all my questions.

Thank you Virgil, Borja, Alessandro and Gabriele for the nice atmosphere in the office. It is nice to work with you in the office.

Thanks to the "coffee break community" for lots of laugh, funny and interesting stories and discussions.

Also thanks to the people of the HOB building 2nd floor contributing to a nice working atmosphere.

I also want to thank my parents and family for the unconditional support during my studies.

Last but not least thanks to Corinna for giving me all the patience, love and happiness. Thanks for all the support.